IOP Publishing Class. Quantum Grav. **43** (2026) 035002 https://doi.org/10.1088/1361-6382/ae3a30

Classical and Quantum Gravity

Check for updates

OPEN ACCESS

RECEIVED
8 October 2025

REVISED
22 December 2025

ACCEPTED FOR PUBLICATION
19 January 2026

PUBLISHED
2 February 2026

Original content from this work may be used under the terms of the Creative Commons Attribution 4.0 licence.

Any further distribution of this work must maintain attribution to the author(s) and the title of the work, journal citation and DOI.

PAPER

Metric-free gravitation from geometrical defects

Jeroen Tromp*

Department of Geosciences and Program in Applied & Computational Mathematics, Princeton University, Princeton, NJ, United States of America

* Author to whom any correspondence should be addressed.

E-mail: jtromp@princeton.edu

Keywords: metric-free gravitation, dislocations, disclinations, point defects, coframe fields, gravitational waves, black holes

Abstract

We develop a metric-free theory of gravitation generated by geometrical defects. Spacetime geometry is described by a *velocity-distortion* coframe $\beta^a = \psi^a{}_\mu \, d\varphi^\mu$ and a *spin-bend-twist* connection $\kappa^a{}_b = \psi^a{}_\mu \, d(\psi^{-1})^\mu{}_b$, defined in terms of the *motion* field φ^μ and the *intrinsic deformation* field $\psi^a{}_\mu$. Their field strengths are the intrinsic torsion $\Sigma^a = d\beta^a + \kappa^a{}_b \wedge \beta^b$ and intrinsic curvature $\Lambda^a{}_b = d\kappa^a{}_b + \kappa^a{}_c \wedge \kappa^c{}_b$. The fundamental field equations $\Sigma^a = \alpha^a$ and $\Lambda^a{}_b = \Theta^a{}_b$ balance these geometric quantities against spacetime *dislocations* α^a and *disclinations* $\Theta^a{}_b$—incompatibilities in the motion and intrinsic deformation fields. Geometrical *point defects* $\Pi^a{}_b$ correspond to incompatible coframe transformations. The Newtonian limit of the time-space field equations $\Lambda^i{}_0 = \Theta^i{}_0$ results in the conversion between the *geometric mass density* $\rho_{\text{geom}} = \iota_{e_i} \iota_u \Theta^i{}_0$ time-space wedge disclination and physical mass-energy ρ. Gravitation thus emerges directly from geometric incompatibility rather than from curvature sourced by matter. An invariant *volume capacity*—a 4-form constructed from orientation and deformation determinants—replaces $\sqrt{-g}$ and enables variational principles and integration without a metric. Variation of an intrinsic-coframe gravitational Lagrangian capacity produces the corresponding stress and couple-stress capacity currents and their dynamical equations. In this formulation, there is no Newtonian gravitational potential: gravitational accelerations are carried by the time-space components of the connection, which act as the fundamental dynamical variables. The theory reproduces gravitational waves, black hole exteriors, and the Newtonian limit in a metric-free formulation; when needed, a metric-compatible sector restriction and metric reconstruction are used only for comparison with standard general relativity. It provides a natural foundation for extensions such as $f(\Lambda)$ theories that may remain valid where metric descriptions fail.

1. Introduction

This paper addresses two fundamental questions: (i) can gravitation be formulated without a metric structure? and (ii) are Einstein's field equations fundamental, or can gravitational phenomena be understood in terms of more elementary geometric structures? We show that core elements usually associated with a metric formulation—field equations, the identification of a Newtonian mass density, gravitational-wave propagation, and analytic black-hole exteriors—can be developed from differential topology and connection geometry alone within the scope of the defect sector treated here. In this framework, the metric tensor—central to general relativity (GR)—is treated as a *derived* object used only for comparison when desired (see 'Metric Comparison' sections), rather than as a fundamental variable.

Observational developments provide further motivation for our understanding of gravitation. The ongoing challenges associated with dark matter and dark energy indicate that a complete understanding of gravitational phenomena across different scales remains elusive (Weinberg 1989, Peebles and Ratra 2003, Bertone and Hooper 2018, Planck Collaboration 2020, Di Valentino *et al* 2021).

© 2026 The Author(s). Published by IOP Publishing Ltd

While these cosmological puzzles motivate exploration of alternative gravitational theories, the minimal model developed here focuses on establishing a coherent metric-free foundation. Extensions necessary to address dark sector phenomena are discussed in section 13.

Precision tests of GR, conducted through gravitational-wave observations (Abbott *et al* 2016, 2017, 2021, 2023, Isi *et al* 2019), confirm the theory's validity in strong-field conditions, although they mainly constrain modifications related to wave propagation rather than offering alternative formulations of the underlying geometric framework.

The perspective of this study aligns with broader efforts in gravitational theory to seek formulations in which connection takes precedence over metric. In particular, work on metric-affine and teleparallel extensions of GR (Trautman 1973, Hehl *et al* 1976, 1995, Aldrovandi and Pereira 2013, Blagojević and Hehl 2013, Hohmann *et al* 2018, Jiménez *et al* 2019, Krssak *et al* 2019, Bahamonde *et al* 2023), including $f(T)$ and $f(Q)$ models (Sotiriou and Faraoni 2010, Capozziello and Laurentis 2011, Järv *et al* 2018, Jiménez *et al* 2018, Lazkoz *et al* 2019, Baldazzi *et al* 2022, Jiménez-Cano 2022, Rigouzzo and Zell 2022, Castillo-Felisola *et al* 2025), has emphasized the role of independent connections and non-Riemannian structures. Connections between GR and gauge theory have also been developed using the Kijowski–Tulczyjew symplectic method (Kijowski and Tulczyjew 1979, Cattaneo and Schiavina 2019). Closely related are proposals that the metric itself emerges from more primitive structures, such as pre-geometry or algebraic gauge frameworks (MacDowell and Mansouri 1977, Wise 2010, Oriti 2014, Addazi *et al* 2025), and pre-metric formulations of field theory (Hehl and Obukhov 2003, Itin 2009).

Our approach contributes to this ongoing discourse by presenting a strictly metric-free theory in which gravitational phenomena emerge directly from incompatibility conditions on motion and intrinsic deformation fields (e.g. Kleinert 1989, 2008).

The present paper develops the *gravitational defect sector* and its vacuum exteriors, and it calibrates the Newtonian mass density identification within that sector. A complete coupling to standard-model matter is not constructed here; this is addressed in section 12 and deferred to follow-on work.

In Einstein's formulation, matter is an external source that curves spacetime, with field equations balancing geometry against stress-energy. By contrast, in the defect-gravity sector developed here, matter is identified with *geometric incompatibility*—regions where spacetime fails to fit together smoothly. The field equations

$$\Sigma^a = \alpha^a, \qquad \Lambda^a{}_b = \Theta^a{}_b,$$

express that intrinsic torsion and curvature, Σ^a and $\Lambda^a{}_b$, are distributionally supported on geometrical defects of spacetime: dislocations α^a and disclinations $\Theta^a{}_b$. Mass emerges specifically as a time-space wedge disclination, a geometric knot between temporal and spatial directions. This interpretation resonates with defect-based and emergent gravity proposals, in which gravitational dynamics are tied to microscopic degrees of freedom or topological excitations (Jacobson 1995, Puntigam and Soleng 1997, Volovik 2003, Padmanabhan 2010, 2012, Barceló *et al* 2011, Liberati 2013, Hossenfelder 2014, Verlinde 2017, Hossenfelder and Gallego Torromé 2018).

The pursuit of metric-free or defect-based gravity has deep historical roots. Cartan introduced torsion as a geometric structure beyond Riemannian curvature (Cartan 1922, 1923), while Einstein briefly explored teleparallel geometry (Einstein 1928). The development of metric-affine gravity and Poincaré gauge theory (Trautman 1973, Hehl *et al* 1976, 1995, Blagojević and Hehl 2013) demonstrated the versatility of connection-based formalisms. Parallel advances in material defect theory (Kondo 1952, 1955, 1963, 1964, Nye 1953, Bilby and Smith 1956, Holländer 1960a, 1960b, 1960c, Noll 1974, Kröner 1981, Mura 1982) established the analogy between dislocations, disclinations, and continuum incompatibilities. Gravitational analogs of defects have been explored in cosmology and condensed matter systems (Katanaev and Volovich 1992, Katanaev 2005, Kleman and Friedel 2008, Carneiro *et al* 2021, Lieu 2024, Adak *et al* 2025, Klinkhamer 2025).

We employ orientation-based volume capacities constructed from deformation determinants, rather than $\sqrt{-g}$, to define invariant integration measures. This enables the construction of a variational principle in which the rest frame mass calibrates the coupling between geometric and physical mass density. The resulting framework reproduces key predictions of GR—including gravitational waves, black hole exteriors, and the Newtonian limit—while offering a new interpretation of matter and gravitation in terms of geometrical defects. By embedding this approach within the broader landscape of metric-affine, pre-metric, and emergent gravity research, we aim to highlight its potential relevance both at classical and quantum scales.

The paper is organized as follows. Section 2 presents the geometrical field equations. Section 3 develops a metric-free description of volume capacities. Section 4 develops the metric-free field theory and derives the Euler–Lagrange balance equations for the constitutive stress currents. Section 5 summarizes the Lagrangian description of gravitation. Section 6 discusses relations to MAG and teleparallel gravity (TEGR). Section 7 shows how gravitational waves emerge from the field equations. Section 8 identifies mass density with time-space disclinations. Section 9 constructs the gravitational Lagrangian encoding mass = geometry. Section 10 presents analytical black hole solutions to the field equations. Section 11 discusses autoparallels. Finally, section 12 discusses implications and section 13 summarizes the results. Appendix A expresses spacetime defects as de Rham currents, and appendix B provides further black hole details.

Occasionally, it will be useful to express results in metric language to make contact with traditional formulations. Such sections are labeled 'Metric Comparison'.

2. Field equations

We begin by introducing the metric-free framework that leads to the geometrical field equations of gravitation.

2.1. Velocity, motion, and intrinsic deformation

A congruence of comoving 'observers' defines a velocity field

$$u \equiv \partial_T\,, \qquad \iota_u \mathrm{d}T = 1\,. \tag{1}$$

In dimensional form, distinguishing the temporal coordinate T from the spatial coordinates $\{X^I\}$, $I = 1,2,3$, requires a universal conversion constant. We work in natural units where this conversion factor is set to unity; its physical value, c, is determined later by identifying the gravitational wave speed with the observed speed of light in section 7.

By analogy with classical continuum mechanics, we refer to the comoving coordinates $\{X^{\mu'}\} = \{T, X^I\}$, $\mu' = 0,1,2,3$ and $I = 1,2,3$, as *Lagrangian coordinates*, which define a Lagrangian chart in the spacetime manifold M. These comoving coordinates complement the standard spacetime coordinates $\{x^\mu\} = \{t, x^i\}$, $\mu = 0,1,2,3$ and $i = 1,2,3$, which are referred to as *Eulerian coordinates*.

In classical continuum mechanics, Lagrangian coordinates are used to label 'particles'; in this context, however, these labels are used to identify members of the congruence of comoving observers.

The Eulerian and Lagrangian coordinates are related via the *motion map*

$$x^\mu = \varphi^\mu\left(X^{\mu'}\right)\,. \tag{2}$$

Since there is a single spacetime manifold M, equipped with both Eulerian and Lagrangian charts, the motion φ is a diffeomorphism on M. The gradient of the motion defines the *deformation gradient*

$$F^\mu{}_{\mu'} \equiv \frac{\partial \varphi^\mu}{\partial X^{\mu'}}\,. \tag{3}$$

An independent intrinsic frame is introduced by the *intrinsic deformation* field

$$\psi^a{}_\mu\left(X^{\mu'}\right) \tag{4}$$

in M. Here, $a = 0,1,2,3$ indexes the intrinsic frame bundle defined at each spacetime event, while $\mu = 0,1,2,3$ refers to the Eulerian chart. The argument $X^{\mu'}$ emphasizes that $\psi^a{}_\mu$ is pulled back to the Lagrangian chart along the congruence of observers. This intrinsic deformation field carries gravity and is analogous to the microrotation (triad/director) field of Cosserat and micropolar elasticity (Cosserat and Cosserat 1907, 1909, Eringen 1999).

We denote the inverse of $\psi^a{}_\mu$ by $(\psi^{-1})^\mu{}_a$, such that $\psi^a{}_\mu(\psi^{-1})^\mu{}_b = \delta^a{}_b$ and $(\psi^{-1})^\mu{}_a\psi^a{}_\nu = \delta^\mu{}_\nu$. For a pure rotation, this would be its transpose. We leave the transformation more general, thereby capturing a wider range of intrinsic deformation.

Thus, as illustrated in figure 1, we consider three coframes in T^*M: the Eulerian coordinate coframe $\mathrm{d}x^\mu$, the Lagrangian coordinate coframe $\mathrm{d}X^{\mu'}$, and the *intrinsic coframe* e^a. These coframes are related via

$$\mathrm{d}x^\mu = F^\mu{}_{\mu'}\,\mathrm{d}X^{\mu'}\,, \qquad e^a = \psi^a{}_\mu\,\mathrm{d}x^\mu = \psi^a{}_\mu F^\mu{}_{\mu'}\,\mathrm{d}X^{\mu'} = e^a{}_{\mu'}\,\mathrm{d}X^{\mu'}\,, \tag{5}$$

where $e^a{}_{\mu'} \equiv \psi^a{}_\mu F^\mu{}_{\mu'}$; we use $e^{\mu'}{}_a$ for its inverse, such that $e^a{}_{\mu'}e^{\mu'}{}_b = \delta^a{}_b$ and $e^{\mu'}{}_a e^a{}_{\nu'} = \delta^{\mu'}{}_{\nu'}$.

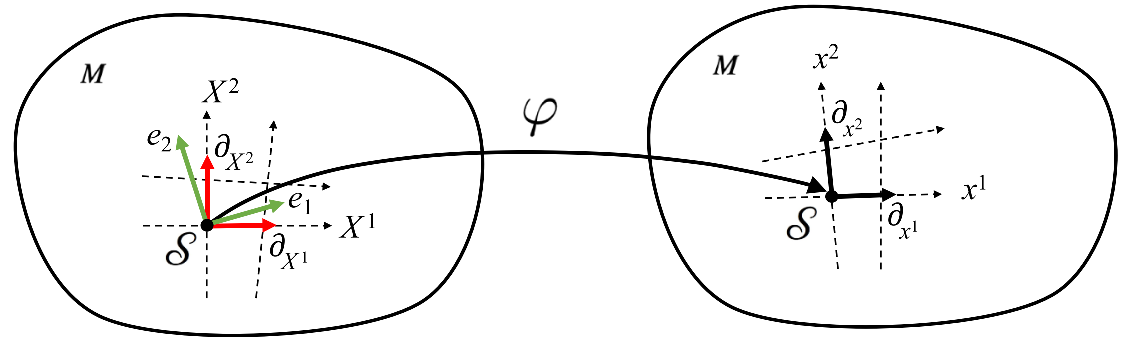

Figure 1. At a spacetime event $\mathscr{S}$ in the spacetime manifold M, we employ three complementary frames. *Right:* in the Eulerian description, an Eulerian chart in M uses coordinates $\{x^\mu\}$ with basis vectors $\{\partial_{x^\mu}\}$ (black arrows). *Left:* In the Lagrangian description, a Lagrangian chart in M uses coordinates $\{X^{\mu'}\}$ with basis vectors $\{\partial_{X^{\mu'}}\}$ (red arrows). Also shown is a coordinate-independent intrinsic frame $\{e_a\}$ (green arrows) with dual coframe $\{e^a\}$. The intrinsic coframe encodes both the macroscopic motion φ^μ and the microscopic deformation $\psi^a{}_\mu$ through the velocity-distortion relation (7), $\beta^a \equiv \psi^a{}_\mu \, \mathrm{d}\varphi^\mu \equiv e^a$. Away from geometrical defects, the Eulerian and Lagrangian charts are smoothly related via the diffeomorphism φ; at defect cores, the motion map φ^μ and the intrinsic deformation $\psi^a{}_\mu$ must be treated distributionally.

To describe their transformation properties we use the full exterior covariant derivative D, which acts on all tensor-valued indices with the appropriate connection: $\Gamma^\mu{}_\nu$ for Eulerian indices, $\Gamma^{\mu'}{}_{\nu'}$ for Lagrangian indices, and $\Gamma^a{}_b$ for intrinsic indices. Compatibility of coframe transformations leads to the standard connection transformation laws

$$\mathrm{D}F^\mu{}_{\mu'} = 0 \iff \Gamma^\mu{}_\nu = F^\mu{}_{\mu'} \Gamma^{\mu'}{}_{\nu'} \left(F^{-1}\right)^{\nu'}{}_\nu + F^\mu{}_{\mu'} \, \mathrm{d}\left(F^{-1}\right)^{\mu'}{}_\nu \,, \tag{6a}$$

$$\mathrm{D}\psi^a{}_\mu = 0 \iff \Gamma^a{}_b = \psi^a{}_\mu \Gamma^\mu{}_\nu \left(\psi^{-1}\right)^\nu{}_b + \psi^a{}_\mu \, \mathrm{d}\left(\psi^{-1}\right)^\mu{}_b \,, \tag{6b}$$

$$\mathrm{D}e^{\mu'}{}_a = 0 \iff \Gamma^{\mu'}{}_{\nu'} = e^{\mu'}{}_a \Gamma^a{}_b e^b{}_{\nu'} + e^{\mu'}{}_a \mathrm{d}e^a{}_{\nu'} \,. \tag{6c}$$

2.2. Velocity-distortion and spin-bend-twist

The vector-valued 1-form

$$\beta^a \equiv \psi^a{}_\mu \, \mathrm{d}\varphi^\mu \tag{7}$$

is the *velocity-distortion coframe*. It encodes both the macroscopic motion φ^μ and the internal microstructural deformation $\psi^a{}_\mu$. The velocity-distortion 1-form defines the intrinsic coframe e^a:

$$\beta^a \equiv e^a \,. \tag{8}$$

Away from defect cores, we assume $\{\beta^a\}$ are linearly independent, so the dual frame $\{e_a\}$ exists with $\beta^a(e_b) = \delta^a{}_b$. This duality provides the basis for contractions ι_{e_a} used throughout the theory.

The intrinsic coframe is endowed with a linear connection

$$\kappa^a{}_b \equiv \psi^a{}_\mu \, \mathrm{d}\left(\psi^{-1}\right)^\mu{}_b = -\left(\psi^{-1}\right)^\mu{}_b \, \mathrm{d}\psi^a{}_\mu \,, \tag{9}$$

called the *spin-bend-twist connection*. It governs parallel transport in the intrinsic bundle and ensures that β^a transforms covariantly.

Together, the velocity-distortion β^a and the spin-bend-twist $\kappa^a{}_b$ are the intrinsic *Lagrangian geometrical potentials* induced by the motion and intrinsic deformation fields $(\varphi^\mu, \psi^a{}_\mu)$.

The nomenclature 'velocity-distortion' and 'spin-bend-twist' is borrowed from continuum mechanics (e.g. deWit 1969, 1973, Kossecka and deWit 1977, Edelen and Lagoudas 1988) because $\iota_u \beta^a = u^a$ is the intrinsic four-*velocity*, $\bar{\beta}^a \equiv \beta^a - u^a \, \mathrm{d}T$ captures the spatial *distortion* of the intrinsic coframe induced by spatial gradients of the motion φ^μ, $\iota_u \kappa^a{}_b \equiv \omega^a{}_b$ is the intrinsic *spin* in the coframe, and $\bar{\kappa}^a{}_b \equiv \kappa^a{}_b - \omega^a{}_b \, \mathrm{d}T$ captures the spatial *bend-twist* of the intrinsic coframe induced by spatial gradients of the intrinsic deformation $\psi^a{}_\mu$. Here, these objects describe the deformation of spacetime coframes themselves; there is no 'ether.'

2.3. Field strengths

The geometric field strengths are the *intrinsic torsion and curvature*

$$\Sigma^a \equiv \mathrm{d}\beta^a + \kappa^a{}_b \wedge \beta^b \equiv \mathscr{D}\beta^a \,, \tag{10a}$$

$$\Lambda^a{}_b \equiv d\kappa^a{}_b + \kappa^a{}_c \wedge \kappa^c{}_b\,, \tag{10b}$$

which vanish identically on any defect-free open set $M \setminus C$. Here $\mathscr{D}$ denotes the exterior covariant derivative involving only the spin-bend-twist connection $\kappa^a{}_b$, and therefore acts only on intrinsic coframe indices a. These are purely differential objects built from β^a and $\kappa^a{}_b$, with no reference to a metric.

Notation. We distinguish three derivative operators:

- d: the exterior derivative;
- D: the exterior covariant derivative acting on all tensor-valued form indices with their appropriate connections ($\Gamma^\mu{}_\nu$ for Eulerian, $\Gamma^{\mu'}{}_{\nu'}$ for Lagrangian, and $\Gamma^a{}_b$ for intrinsic indices);
- $\mathscr{D}$: the covariant exterior derivative built solely from the spin-bend-twist connection $\kappa^a{}_b$.

2.4. Intrinsic Bianchi identities

The intrinsic torsion (10*a*) and curvature (10*b*) satisfy the intrinsic Bianchi identities

$$\mathscr{D}\Sigma^a = \Lambda^a{}_b \wedge \beta^b\,, \qquad \mathscr{D}\Lambda^a{}_b = 0\,. \tag{11}$$

These express the Lagrangian *compatibility conditions* of the intrinsic coframe.

2.5. Defects

Geometrical incompatibilities appear as defect densities:

- *Dislocations:*

$$\alpha^a \equiv \psi^a{}_\mu\, d^2\varphi^\mu \quad (\text{failure of motion-field compatibility})\,, \tag{12}$$

  which serve as sources of intrinsic torsion Σ^a.
- *Disclinations:*

$$\Theta^a{}_b \equiv -\left(d^2\psi^a{}_\mu\right)\left(\psi^{-1}\right)^\mu{}_b \quad (\text{failure of intrinsic-deformation-field compatibility})\,, \tag{13}$$

  which serve as sources of intrinsic curvature $\Lambda^a{}_b$.
- *Point defects:*

$$\begin{aligned}\Pi^a{}_b &= (D\psi^a{}_\mu)\left(\psi^{-1}\right)^\mu{}_b \\ &= (d\psi^a{}_\mu + \Gamma^a{}_c\psi^c{}_\mu - \psi^a{}_\nu\Gamma^\nu{}_\mu)\left(\psi^{-1}\right)^\mu{}_b \\ &= \Gamma^a{}_b - \psi^a{}_\nu\Gamma^\nu{}_\mu\left(\psi^{-1}\right)^\mu{}_b - \kappa^a{}_b\,,\end{aligned} \tag{14}$$

  arising from a discontinuous coframe transformation (6*b*). Defining the 'good' connection

$$\Omega^a{}_b \equiv \psi^a{}_\nu\Gamma^\nu{}_\mu\left(\psi^{-1}\right)^\mu{}_b + \kappa^a{}_b\,, \tag{15}$$

  we see that $\Pi^a{}_b = \Gamma^a{}_b - \Omega^a{}_b$ is the difference between two connections, and therefore tensorial.

Definitions (12) and (13) are understood in the sense of de Rham currents (De Rham 1955): $d^2 = 0$ for smooth forms, but when φ^μ or $\psi^a{}_\mu$ carry distributional support, their first derivatives already contain Dirac measures and their second exterior derivatives define non-zero currents supported on defect cores C, as discussed in appendix A.

2.5.1. Metric comparison

If a metric is reconstructed from the coframe according to

$$g = g_{ab}\,\beta^a \otimes \beta^b\,, \qquad g_{\mu\nu} = g_{ab}\,\psi^a{}_\mu\,\psi^b{}_\nu\,, \tag{16}$$

then the metric-affine nonmetricity (e.g. Hehl *et al* 1995, Hehl and Obukhov 2003, Bahamonde *et al* 2023)

$$Q_{\mu\nu} = -Dg_{\mu\nu} \tag{17}$$

is related to the point defect tensor via

$$Q_{\mu\nu} = -\left[Dg_{ab} + 2\Pi_{(ab)}\right]\psi^a{}_\mu\,\psi^b{}_\nu \tag{18}$$

where $\Pi_{ab} \equiv g_{ac}\Pi^c{}_b$. Hence, the usual MAG nonmetricity (17) corresponds to the symmetric part of the intrinsic point-defect tensor plus the *intrinsic nonmetricity*

$$q_{ab} = -\mathrm{D}g_{ab}\,. \tag{19}$$

The symmetric part of the point defect tensor, therefore, captures both background and intrinsic nonmetricity:

$$\Pi_{(ab)} = \tfrac{1}{2}\left[q_{ab} - Q_{\mu\nu}\left(\psi^{-1}\right)^{\mu}{}_{a}\left(\psi^{-1}\right)^{\nu}{}_{b}\right]. \tag{20}$$

The failure of coframe compatibility is encoded entirely in $\Pi^a{}_b$; according to (18), its symmetric part plays the role of nonmetricity, while its antisymmetric part represents an intrinsically new sector not visible in MAG:

$$\Pi^a{}_b = \tfrac{1}{4}\,\delta^a{}_b\,\Pi^c{}_c + \left[\Pi^{(a}{}_{b)} - \tfrac{1}{4}\,\delta^a{}_b\,\Pi^c{}_c\right] + \Pi^{[a}{}_{b]}\,, \tag{21}$$

with trace (dilatational), symmetric-traceless (shear), and antisymmetric (spin) parts.

2.6. Field equations

The intrinsic torsion and curvature are *defined* by the Cartan structure equations (10*a*) and (10*b*). In defect-free regions where (φ,ψ) are smooth, these compatibility relations yield $\Sigma^a = 0$ and $\Lambda^a{}_b = 0$. As discussed in section 2.5, defects are introduced by allowing (φ,ψ) to carry singular support on a set C, so that Σ^a and $\Lambda^a{}_b$ become de Rham currents supported on C; we denote these defect currents by α^a and $\Theta^a{}_b$ and write

$$\Sigma^a = \alpha^a\,, \qquad \Lambda^a{}_b = \Theta^a{}_b\,. \tag{22}$$

These field equations express that intrinsic torsion and curvature are *distributionally supported* on defects. Here 'distributionally supported' is understood in the sense of de Rham currents, so that intrinsic torsion and curvature vanish as smooth forms on $U = M\setminus C$ but carry singular support on the defect set C. In a defect-free region U one has $\Sigma^a = 0$ and $\Lambda^a{}_b = 0$. Hence, gravitational phenomena are interpreted as manifestations of the geometric incompatibilities encoded in these defect distributions.

2.7. Coframe torsion and curvature

The full coframe torsion and curvature decompose into smooth and intrinsic (defect) parts:

$$T^a = \mathrm{d}\beta^a + \Gamma^a{}_b\wedge\beta^b \tag{23a}$$

$$= \psi^a{}_\mu\,T^\mu + \Sigma^a + \Pi^a{}_b\wedge\beta^b\,, \tag{23b}$$

and

$$R^a{}_b = \mathrm{d}\Gamma^a{}_b + \Gamma^a{}_c\wedge\Gamma^c{}_b \tag{24a}$$

$$= \psi^a{}_\mu\,R^\mu{}_\nu\left(\psi^{-1}\right)^\nu{}_b + \Lambda^a{}_b + \mathrm{D}\Pi^a{}_b + \Pi^a{}_c\wedge\Pi^c{}_b\,, \tag{24b}$$

where intrinsic torsion Σ^a, intrinsic curvature $\Lambda^a{}_b$, and point defects $\Pi^a{}_b$ are supported on the defect core C. Thus, on any smooth, defect-free region U one has $\Sigma^a = 0$, $\Lambda^a{}_b = 0$, and $\Pi^a{}_b = 0$, and

$$T^a\big|_U = \psi^a{}_\mu\,T^\mu\,, \qquad R^a{}_b\big|_U = \psi^a{}_\mu\,R^\mu{}_\nu\left(\psi^{-1}\right)^\nu{}_b\,. \tag{25}$$

To summarize the notation: we reserve Σ^a, $\Lambda^a{}_b$ for *intrinsic* torsion and curvature (computed from $\kappa^a{}_b$); T^a, $R^a{}_b$ for the *full coframe* torsion and curvature (computed from $\Gamma^a{}_b$).

2.8. Defect Bianchi identities

The concept of exterior differentiation applies to de Rham currents, which allows for a distributional interpretation of the intrinsic Bianchi identities. When defect cores are idealized as distributions, the identities expressed in equation (11) are understood in a regularized manner. Specifically, these identities hold pointwise for the smooth family $(\beta^a_\varepsilon, \kappa^a{}_{b,\varepsilon})$. The current identity is then derived by taking the limit as ε approaches zero after forming the wedge products at the smooth level.

In this sense, $\mathscr{D}^2 = \Lambda$ and $\mathscr{D}\Lambda = 0$ continue to hold even when β^a and $\kappa^a{}_b$ carry singular support on defect cores. Thus, substituting the field equations $\Sigma^a = \alpha^a$ and $\Lambda^a{}_b = \Theta^a{}_b$ into (11) yields the distributional defect Bianchi identities:

$$\mathscr{D}\alpha^a = \Theta^a{}_b\wedge\beta^b\,, \qquad \mathscr{D}\Theta^a{}_b = 0\,. \tag{26}$$

These express the compatibility relations among dislocations, disclinations, and the velocity-distortion in the Lagrangian framework. Equation (26) are four-dimensional *compatibility conditions*, equivalent to the compatibility conditions for material defects (e.g. deWit 1969, 1973, Kossecka and deWit 1977, Edelen and Lagoudas 1988, Kleman and Friedel 2008).

3. Volume capacities

In the absence of a metric, invariant integration measures may be constructed from orientation, the alternating symbol, and the determinants of the deformation maps $F^{\mu}{}_{\mu'}$ and $\psi^{a}{}_{\mu}$. This yields a *volume capacity*—a differential form that transforms with the Jacobians of F or ψ, rather than with metric determinants.

On the spacetime manifold M, the oriented 4-form capacity is

$$\begin{aligned} \epsilon &= \tfrac{1}{4!}\,\varepsilon_{\mu\nu\tau\sigma}\,\mathrm{d}x^{\mu}\wedge\mathrm{d}x^{\nu}\wedge\mathrm{d}x^{\tau}\wedge\mathrm{d}x^{\sigma} \\ &= \tfrac{1}{4!}\,F\varepsilon_{\mu'\nu'\tau'\sigma'}\,\mathrm{d}X^{\mu'}\wedge\mathrm{d}X^{\nu'}\wedge\mathrm{d}X^{\tau'}\wedge\mathrm{d}X^{\sigma'} \\ &= \tfrac{1}{4!}\,\psi^{-1}\,\varepsilon_{abcd}\,\beta^{a}\wedge\beta^{b}\wedge\beta^{c}\wedge\beta^{d}\,, \end{aligned} \tag{27}$$

where F and ψ play the role of intrinsic Jacobians:

$$F \equiv \tfrac{1}{4!}\,\varepsilon_{\mu\nu\tau\sigma}\,F^{\mu}{}_{\mu'}F^{\nu}{}_{\nu'}F^{\tau}{}_{\tau'}F^{\sigma}{}_{\sigma'}\,\varepsilon^{\mu'\nu'\tau'\sigma'}\,, \tag{28}$$

$$\psi \equiv \tfrac{1}{4!}\,\varepsilon_{abcd}\,\psi^{a}{}_{\mu}\,\psi^{b}{}_{\nu}\,\psi^{c}{}_{\tau}\,\psi^{d}{}_{\sigma}\,\varepsilon^{\mu\nu\tau\sigma}\,. \tag{29}$$

Here $\varepsilon_{\mu\nu\tau\sigma}$, $\varepsilon^{\mu'\nu'\tau'\sigma'}$, ε_{abcd}, and ε^{abcd} are alternating symbols (densities and capacities), defined by $\varepsilon_{0123}=+1$ and $\varepsilon^{0123}=+1$ in positively oriented charts; upper/lower positions do not involve a metric. F and ψ are oriented Jacobians; they change sign under orientation-reversing transformations. Thus, the Eulerian, Lagrangian, and intrinsic constructions all realize the same idea: oriented volume capacities can be defined without a metric, relying only on alternating symbols and deformation determinants.

3.1. Cascade of volume capacities

Following, e.g., Hehl and Obukhov (2003), it is convenient to introduce the completely antisymmetric capacity[2]

$$\epsilon_{abcd} \equiv \psi^{-1}\,\varepsilon_{abcd}\,, \tag{30}$$

so that the oriented 4-form capacity takes the compact form

$$\epsilon = \tfrac{1}{4!}\,\epsilon_{abcd}\,\beta^{a}\wedge\beta^{b}\wedge\beta^{c}\wedge\beta^{d}\,, \tag{31}$$

where β^{a} denotes the velocity-distortion, which equals the intrinsic coframe e^{a}. From this, one obtains a cascade of lower-rank capacities (a metric-free version of Trautman 1973)

$$\epsilon_{a} \equiv \tfrac{1}{3!}\,\epsilon_{abcd}\,\beta^{b}\wedge\beta^{c}\wedge\beta^{d}\,, \tag{32a}$$

$$\epsilon_{ab} \equiv \tfrac{1}{2!}\,\epsilon_{abcd}\,\beta^{c}\wedge\beta^{d}\,, \tag{32b}$$

$$\epsilon_{abc} \equiv \epsilon_{abcd}\,\beta^{d}\,. \tag{32c}$$

These satisfy the wedge identities

$$\beta^{c}\wedge\epsilon_{abd} = \delta^{c}{}_{d}\,\epsilon_{ab} + \delta^{c}{}_{b}\,\epsilon_{da} + \delta^{c}{}_{a}\,\epsilon_{bd}\,, \tag{33a}$$

$$\beta^{c}\wedge\epsilon_{ab} = \delta^{c}{}_{a}\,\epsilon_{b} - \delta^{c}{}_{b}\,\epsilon_{a}\,, \tag{33b}$$

$$\beta^{b}\wedge\epsilon_{a} = \delta^{b}{}_{a}\,\epsilon\,. \tag{33c}$$

[2] There is an equivalent definition in the Lagrangian coframe: $\epsilon_{\mu'\nu'\tau'\sigma'} \equiv F\varepsilon_{\mu'\nu'\tau'\sigma'}$, with a corresponding cascade.

3.2. Observer-sliced 3D and 2D capacities

Given a choice of time-flow u with $u^a \equiv \iota_u \beta^a$ and $\iota_u \mathrm{d}T = 1$, we define the spatial (3D) volume capacity and its (2D) surface cascade by

$$\hat{\epsilon} \equiv \iota_u \epsilon , \qquad \hat{\epsilon}_a \equiv \iota_{e_a} \hat{\epsilon} = \iota_{e_a} \iota_u \epsilon . \tag{34}$$

Using the cascade ϵ_a one has the general identities

$$\hat{\epsilon} = u^a \epsilon_a , \qquad \beta^a \wedge \hat{\epsilon} = u^a \epsilon , \qquad \beta^b \wedge \hat{\epsilon}_a = u^c \beta^b \wedge \iota_{e_a} \epsilon_c = \delta^b{}_a \hat{\epsilon} - u^b \epsilon_a , \tag{35}$$

where the last equality follows from (33*b*)–(33*c*) and $\iota_{e_a}\epsilon_c = -\iota_{e_c}\epsilon_a$. In a u-adapted frame with $u^a = \delta^a{}_0$, these reduce to

$$\beta^0 \wedge \hat{\epsilon} = \epsilon , \quad \beta^i \wedge \hat{\epsilon}_j = \delta^i{}_j \hat{\epsilon} , \quad \beta^0 \wedge \hat{\epsilon}_i = -\epsilon_i , \quad \iota_{e_0} \hat{\epsilon} = 0 , \quad \iota_{e_0} \hat{\epsilon}_i = 0 , \quad (i,j = 1,2,3) , \tag{36}$$

which mirrors the usual 'spatial area times spatial normal' structure, derived purely from the capacity cascade and the chosen time-flow.

The cascade of capacities introduced here provides the universal integration measures in the absence of a metric. They will reappear throughout the theory: (a) as the foundation of the general Lagrangian framework in section 4, where L is taken to be a 4-form capacity; (b) in the identification of mass density with time-space disclinations in section 8, where spatial capacities $\hat{\epsilon}$ and $\hat{\epsilon}_i$ are used to define intrinsic fluxes; and (c) in the construction of the specific gravitational Lagrangian of section 9, where the time-flow u and the 2-form capacities ϵ_{ab} determine energetic couplings to curvature; (d) in the analysis of black hole exteriors in section 10, where the orbit area capacity σ provides the intrinsic definition of areal radius and horizon area. Thus, all subsequent constructions of dynamics, sources, and solutions rest on these metric-free volume capacities.

4. Field theory

In this section, we introduce a metric-free intrinsic-coframe variational framework based on a *Lagrangian capacity* L, i.e. a 4-form constructed directly from the intrinsic geometric fields. In analogy with metric theories, where the action is a scalar Lagrangian density multiplied by a metric volume element, here the fundamental variational object is itself a 4-form capacity. Consequently, all variational derivatives are naturally 3-form capacities, in precise analogy with the cascade of volume capacities introduced in section 3. The action

$$S = \int_M L \tag{37}$$

is therefore coordinate-invariant without reference to a metric.

4.1. Kinematics, gauge potentials, and tensorial dependence

The defect formulation is built from the motion field φ^μ and the intrinsic deformation field $\psi^a{}_\mu$, through which we define the velocity-distortion coframe β^a and the spin-bend-twist connection $\kappa^a{}_b$ according to (7) and (9). The connection $\kappa^a{}_b$ is not tensorial, but the field theory depends on the gauge potentials (φ,ψ) only through the tensorial intrinsic field strengths Σ^a and $\Lambda^a{}_b$, given by (10*a*) and (10*b*), together with β^a itself. Accordingly, the Lagrangian capacity is taken to be

$$L = L(\beta^a, \Sigma^a, \Lambda^a{}_b, \Pi^a{}_b) \equiv L(\beta^a(\varphi,\psi), \Sigma^a(\varphi,\psi), \Lambda^a{}_b(\varphi,\psi), \Pi^a{}_b(\varphi,\psi)) , \tag{38}$$

so that the action is invariant under changes of intrinsic basis (local gauge transformations) and does not require a metric.

4.2. Constitutive stresses as variational response

Although L depends on (φ,ψ) only through tensorial quantities, it is convenient to compute its first variation using $\delta\beta^a$ and $\delta\kappa^a{}_b$, which are induced by $(\delta\varphi,\delta\psi)$ through (7) and (9). From (10*a*) and (10*b*), we obtain

$$\delta\Sigma^a = \mathscr{D}\delta\beta^a + \delta\kappa^a{}_b \wedge \beta^b , \qquad \delta\Lambda^a{}_b = \mathscr{D}\delta\kappa^a{}_b , \tag{39}$$

where $\mathscr{D}$ denotes the intrinsic covariant exterior derivative built from $\kappa^a{}_b$. This yields the standard first-variation identity

$$\delta L = \delta\beta^a \wedge \sigma_a + \delta\kappa^a{}_b \wedge \tau_a{}^b + \delta\Pi^a{}_b \wedge \pi_a{}^b + \mathrm{d}\left(\delta\beta^a \wedge \frac{\partial L}{\partial \Sigma^a} + \delta\kappa^a{}_b \wedge \frac{\partial L}{\partial \Lambda^a{}_b}\right), \tag{40}$$

where we define the *Lagrangian stress* 3-form capacities by

$$\sigma_a \equiv \frac{\partial L}{\partial \beta^a} + \mathscr{D}\frac{\partial L}{\partial \Sigma^a}, \tag{41}$$

the *Lagrangian couple-stress* 3-form capacities by

$$\tau_a{}^b \equiv \mathscr{D}\frac{\partial L}{\partial \Lambda^a{}_b} + \beta^b \wedge \frac{\partial L}{\partial \Sigma^a}, \tag{42}$$

and the *Lagrangian point-stress* 3-form capacities by

$$\pi_a{}^b \equiv \frac{\partial L}{\partial \Pi^a{}_b}. \tag{43}$$

These 3-form capacities are not set to zero in general; rather, they are constitutive response currents determined by L and evaluated on the kinematics (7) and (9).

4.3. Euler–Lagrange equations for the gauge potentials

Following the standard Cosserat (micropolar) continuum-mechanics viewpoint, we take the *gauge potentials*–the motion φ^μ and the intrinsic distortion $\psi^a{}_\mu$–as the fundamental variables (e.g. Eringen 1999). The action is defined by stationarity with respect to compactly supported variations $\delta\varphi^\mu$ and $\delta\psi^a{}_\mu$ (or, equivalently, by imposing boundary conditions that eliminate total-derivative terms).

Induced variations. Because β^a and $\kappa^a{}_b$ are induced by (φ, ψ) through (7) and (9), the variations $\delta\beta^a$ and $\delta\kappa^a{}_b$ are not independent.

For a variation $\delta\varphi^\mu$ of the motion field, we introduce the associated virtual-displacement vector field ξ on $M \setminus C$ by requiring[3]

$$\delta\varphi^\mu = \iota_\xi \, \mathrm{d}\varphi^\mu. \tag{44}$$

And define its intrinsic components

$$\xi^a \equiv \iota_\xi \beta^a = \psi^a{}_\mu \delta\varphi^\mu. \tag{45}$$

For a variation $\delta\psi^a{}_\mu$ of the intrinsic deformation field, define the 0-form

$$\chi^a{}_b \equiv \delta\psi^a{}_\mu \left(\psi^{-1}\right)^\mu{}_b + \iota_\xi \kappa^a{}_b. \tag{46}$$

The combination of terms on the right-hand side is the gauge-covariant variation: it packages the intrinsic frame change together with the connection term generated by transport along ξ.

With these definitions, the induced variations of the intrinsic potentials take the covariant form

$$\delta\beta^a = \mathscr{D}\xi^a + \chi^a{}_b \beta^b + \iota_\xi \Sigma^a, \tag{47a}$$

$$\delta\kappa^a{}_b = \mathscr{D}\chi^a{}_b + \iota_\xi \Lambda^a{}_b, \tag{47b}$$

$$\delta\Pi^a{}_b = \mathscr{D}\left(\iota_\xi \Pi^a{}_b\right) + \iota_\xi\left(\mathscr{D}\Pi^a{}_b\right) + \chi^a{}_c \Pi^c{}_b - \Pi^a{}_c \chi^c{}_b, \tag{47c}$$

where $\mathscr{D}$ is the intrinsic covariant exterior derivative built from $\kappa^a{}_b$. Equations (47a)–(47b) follow from Cartan's formula for the Lie derivative applied to (7) and (9), together with the definitions of Σ^a and $\Lambda^a{}_b$. Equivalently, (47a)–(47b) are the intrinsic, metric-free counterparts of Cartan's variation formulas for the Lie derivative of gauge potentials: the $(\xi^a, \chi^a{}_b)$ decomposition separates virtual transport along ξ from an intrinsic frame variation χ. Equation (47c) is the corresponding intrinsic Cartan variation for the tensor-valued 1-form $\Pi^a{}_b$: it combines virtual transport along ξ with the adjoint action of the intrinsic frame variation χ.

[3] For a 0-form φ^μ, $\mathcal{L}_\xi \varphi^\mu = \iota_\xi \, \mathrm{d}\varphi^\mu$.

Variation of the action in terms of (ξ,χ). We insert (47) into the first-variation identity (40) and discard total derivatives using the assumed support/boundary conditions. Using $\iota_\xi\Sigma^a = \xi^c\,\iota_{e_c}\Sigma^a$ and $\iota_\xi\Lambda^a{}_b = \xi^c\,\iota_{e_c}\Lambda^a{}_b$, we obtain

$$\delta S = \int_M \{(\mathscr{D}\xi^a)\wedge\sigma_a + (\mathscr{D}\chi^a{}_b)\wedge\tau_a{}^b + \chi^a{}_b\,\beta^b\wedge\sigma_a + \xi^c\,(\iota_{e_c}\Sigma^a)\wedge\sigma_a + \xi^c\,(\iota_{e_c}\Lambda^a{}_b)\wedge\tau_a{}^b \\ + [\mathscr{D}(\iota_\xi\,\Pi^a{}_b)]\wedge\pi_a{}^b + \xi^c\,(\iota_{e_c}\mathscr{D}\Pi^a{}_b)\wedge\pi_a{}^b + \chi^a{}_c\,\Pi^c{}_b\wedge\pi_a{}^b - \Pi^a{}_c\,\chi^c{}_b\wedge\pi_a{}^b\}\,. \tag{48}$$

Now integrate by parts covariantly, using $\mathscr{D}(\xi^a\sigma_a) = (\mathscr{D}\xi^a)\wedge\sigma_a + \xi^a\mathscr{D}\sigma_a$ and similarly for $\mathscr{D}(\chi^a{}_b\tau_a{}^b)$, and using $\mathscr{D}\left[(\iota_\xi\,\Pi^a{}_b)\,\pi_a{}^b\right] = [\mathscr{D}(\iota_\xi\,\Pi^a{}_b)]\wedge\pi_a{}^b + (\iota_\xi\,\Pi^a{}_b)\,\mathscr{D}\pi_a{}^b$, again discarding boundary terms. This yields

$$\delta S = -\int_M \{\xi^a\left[\mathscr{D}\sigma_a - \left(\iota_{e_a}\Sigma^b\right)\wedge\sigma_b - \left(\iota_{e_a}\Lambda^b{}_c\right)\wedge\tau_b{}^c - \left(\iota_{e_a}\mathscr{D}\Pi^c{}_d\right)\wedge\pi_c{}^d + \left(\iota_{e_a}\Pi^c{}_d\right)\mathscr{D}\pi_c{}^d\right] \\ + \chi^a{}_b\left(\mathscr{D}\tau_a{}^b - \sigma_a\wedge\beta^b + \Pi^b{}_c\wedge\pi_a{}^c - \pi_c{}^b\wedge\Pi^c{}_a\right)\}\,. \tag{49}$$

Here we used definitions (42) and (43), and we collected the point-defect contributions carried by $\Pi^a{}_b$ and its response current $\pi_a{}^b$.

Euler–Lagrange balance equations. Since $(\delta\varphi,\delta\psi)$ are arbitrary (with the stated support/boundary conditions), the induced 0-forms $(\xi^a,\chi^a{}_b)$ may be taken arbitrary and independent. Stationarity $\delta S = 0$ therefore implies the balance equations

$$\mathscr{D}\sigma_a = \left(\iota_{e_a}\Sigma^b\right)\wedge\sigma_b + \left(\iota_{e_a}\Lambda^b{}_c\right)\wedge\tau_b{}^c + \left(\iota_{e_a}\mathscr{D}\Pi^c{}_d\right)\wedge\pi_c{}^d - \left(\iota_{e_a}\Pi^c{}_d\right)\mathscr{D}\pi_c{}^d\,, \tag{50a}$$

$$\mathscr{D}\tau_a{}^b = \sigma_a\wedge\beta^b - \Pi^b{}_c\wedge\pi_a{}^c + \pi_c{}^b\wedge\Pi^c{}_a\,. \tag{50b}$$

4.4. Distributional defect sources and variational consistency

In applications, the fields (φ,ψ)–and hence $(\beta^a,\kappa^a{}_b)$–are typically smooth on $M\setminus C$ and may be singular on a defect set $C\subset M$ (e.g. a timelike worldsheet) in the sense described in appendix A. Accordingly, Σ^a and $\Lambda^a{}_b$ may be interpreted as de Rham currents supported on C.

To justify the variational manipulations in the preceding subsections in the presence of such singularities, we use a standard *regularize-vary-limit* procedure[4].

Let $(\varphi_\varepsilon,\psi_\varepsilon)$ be a regularized defect-core family (appendix A.3) with smooth induced fields $(\beta^a_\varepsilon,\kappa^a{}_{b,\varepsilon})$ and smooth field strengths $(\Sigma^a_\varepsilon,\Lambda^a{}_{b,\varepsilon},\Pi^a{}_{b,\varepsilon})$ for each $\varepsilon>0$. Define the regularized action

$$S_\varepsilon \equiv \int_M L\,(\beta^a_\varepsilon,\Sigma^a_\varepsilon,\Lambda^a{}_{b,\varepsilon},\Pi^a{}_{b,\varepsilon})\,. \tag{51}$$

For each fixed $\varepsilon>0$ the derivation leading to (40) is classical, and yields

$$\delta S_\varepsilon = \int_M \delta\beta^a\wedge\sigma_{a,\varepsilon} + \delta\kappa^a{}_b\wedge\tau_{a,\varepsilon}{}^b + \delta\Pi^a{}_b\wedge\pi_{a,\varepsilon}{}^b + \mathrm{d}(\cdots)\,, \tag{52}$$

with $(\sigma_{a,\varepsilon},\tau_{a,\varepsilon}{}^b,\pi_{a,\varepsilon}{}^b)$ defined exactly as in (41)–(43) and evaluated on the regularized fields.

Admissible variations $(\delta\varphi,\delta\psi)$ are taken smooth and compactly supported in M (or subject to boundary conditions eliminating total derivatives), so that $\int_M \mathrm{d}(\cdots) = 0$ for each fixed $\varepsilon>0$. Stationarity $\delta S_\varepsilon = 0$ for all admissible $(\delta\varphi,\delta\psi)$ is then equivalent to the smooth balance equations (50a)–(50b) with all fields replaced by their ε-regularized counterparts.

Finally, we define the singular (defect) action by the current limit

$$S \equiv \lim_{\varepsilon\to 0} S_\varepsilon\,, \tag{53}$$

and interpret the Euler–Lagrange equations in the *distributional (current) sense* by taking $\varepsilon\to 0$ after variation. Concretely, for any smooth compactly supported test 0-forms $(\xi^a,\chi^a{}_b)$ (equivalently, admissible $(\delta\varphi,\delta\psi)$ through (44) and (46)), the condition $\delta S = 0$ is understood as

$$0 = \delta S \equiv \lim_{\varepsilon\to 0}\delta S_\varepsilon = -\lim_{\varepsilon\to 0}\int_M \left(\xi^a\,\mathcal{E}_{a,\varepsilon} + \chi^a{}_b\,\mathcal{E}_{a,\varepsilon}{}^b\right)\,, \tag{54}$$

[4] The point is that all products and integrations by parts are carried out at fixed $\varepsilon>0$ in the smooth category, and only then is the current limit taken; this avoids undefined products of distributions. See, e.g. Geroch and Traschen (1987), Federer (1996), Giaquinta *et al* (1998), and Krantz and Parks (2008) for standard formulations of weak/current limits and controlled regularization.

where $\mathcal{E}_{a,\varepsilon}$ and $\mathcal{E}_{a,\varepsilon}{}^{b}$ are the ε-regularized residuals appearing in the parentheses in (49). In this sense, the limiting fields satisfy the balance equations (50*a*) and (50*b*) as de Rham currents on M, with defect-supported contributions encoded by the current limits of $(\Sigma^a_\varepsilon, \Lambda^a{}_{b,\varepsilon}, \Pi^a{}_{b,\varepsilon})$.

Equations (50*b*) and (50*a*) are the Euler–Lagrange equations for the gauge potentials (φ, ψ), expressing covariant balance of the constitutive stress, couple-stress, and point-stress currents induced by the intrinsic geometry. In particular, defect-supported curvature and torsion enter (50*a*) and (50*b*) through the current limits of $(\Sigma^a_\varepsilon, \Lambda^a{}_{b,\varepsilon}, \Pi^a{}_{b,\varepsilon})$, so that localized defects act as intrinsic sources of stress without introducing an external matter Lagrangian.

5. Summary of the Lagrangian description

The metric-free Lagrangian theory is summarized in table 1. No dimensionful constants enter the theory until two physical calibrations are imposed. First, the universal signal speed introduced in the kinematic formulation is identified in section 7 as the propagation speed of gravitational disturbances, thereby acquiring its empirical interpretation as the speed of light c. Second, in section 8, the relation between physical and geometric mass density is fixed in the Newtonian limit, introducing the gravitational constant G. Together, these identifications establish the bridge between purely geometric quantities and measurable physical units. Thus, geometry determines structure, while calibration determines scale.

6. Metric comparison: relation to metric-affine and TEGR

This section explores the metric-free defect formulation within the wider context of connection-based gravity. It is included specifically to establish connections with MAG and teleparallel formulations of GR (e.g. Trautman 1973, Hehl *et al* 1976, 1995, Aldrovandi and Pereira 2013, Blagojević and Hehl 2013, Hohmann *et al* 2018, Jiménez *et al* 2019, Krssak *et al* 2019, Bahamonde *et al* 2023). Throughout the paper, the primary variables are the velocity-distortion coframe β^a and the spin-bend-twist connection $\kappa^a{}_b$, along with their corresponding Euler–Lagrange balance equations.

6.1. Metric-affine points of contact

In the context of MAG, one typically works with an independent metric g (or an independent coframe e^a alongside a metric in the internal space) and an independent affine connection. From these components, one can define torsion T^a, curvature $R^a{}_b$, and nonmetricity $Q_{ab} \equiv -Dg_{ab}$.

In contrast, within the current framework, g is not regarded as a fundamental entity. Instead, the gauge potentials are represented as $(\varphi^\mu, \psi^a{}_\mu)$, which give rise to the intrinsic geometric potentials $(\beta^a, \kappa^a{}_b)$. The operative gravitational degrees of freedom are determined by the associated incompatibilities, namely intrinsic torsion and curvature.

However, a metric can still be reconstructed for comparative purposes by choosing an internal bilinear form (for example, η_{ab}) and defining $g \equiv \eta_{ab}\beta^a \otimes \beta^b$. It is important to note that this reconstructed metric is a derived comparison object, rather than a defining structure.

6.2. Teleparallel and symmetric-teleparallel limits

TEGR is defined by having zero curvature and non-zero torsion, while symmetric TEGR is characterized by zero torsion and curvature but with non-zero nonmetricity. Within the current framework, these correspond to *restricted sectors* that arise from imposing additional constraints on $(\Sigma^a, \Lambda^a{}_b)$ (and, if one decides to reconstruct g, on the induced nonmetricity).

In particular, the defect currents $(\alpha^a, \Theta^a{}_b, \Pi^a{}_b)$ offer a natural distributional generalization of these restricted sectors. This means that the corresponding field strengths can vanish outside of the set $M \setminus C$ while still exhibiting non-trivial holonomy or flux that is concentrated around the defect cores.

6.3. What is new in the present framework

The primary distinctions compared to standard MAG/teleparallel formalisms are as follows: (i) The use of a metric-free integration measure based on volume capacities. (ii) The identification of sources through geometric incompatibilities, which are treated as de Rham currents. (iii) An intrinsic Lagrangian-capacity variational structure that produces stress, couple-stress, and point-stress as 3-form capacities, along with their corresponding Euler–Lagrange balance equations, without the need to introduce $\sqrt{-g}$ or a Newtonian potential. These distinctions are summarized in table 2.

Table 1. Summary of the Lagrangian description of gravitation. Gauge potentials are the motion φ^μ and the intrinsic distortion $\psi^a{}_\mu$, which induce the velocity-distortion 1-forms $\beta^a = \psi^a{}_\mu\, \mathrm{d}\varphi^\mu$ and the spin-bend-twist connection 1-forms $\kappa^a{}_b = \psi^a{}_\mu\, \mathrm{d}(\psi^{-1})^\mu{}_b$. Field strengths are the intrinsic torsion 2-forms Σ^a and intrinsic curvature 2-forms $\Lambda^a{}_b$, linked by Bianchi identities. The covariant exterior derivative $\mathscr{D}$ involves the spin-bend-twist connection 1-forms $\kappa^a{}_b$. Incompatibilities in the motion φ^μ produce geometrical dislocations α^a, and incompatibilities in the intrinsic deformation $\psi^a{}_\mu$ produce geometrical disclinations $\Theta^a{}_b$. Incompatible coframe transformations give rise to point defects $\Pi^a{}_b$. The terms $\mathrm{d}^2\varphi^\mu$ and $\mathrm{d}^2\psi^a{}_\mu$ are interpreted as de Rham currents or distributions (see appendix A. The field equations support linearized gravitational waves, yield Poisson's equation in the Newtonian limit, and admit analytical black hole solutions. The intrinsic Lagrangian is a 4-form capacity L, whose variations yield Lagrangian stress, couple stress, and point stress *3-form capacities*. These are the natural conjugates to Σ^a, $\Lambda^a{}_b$, and $\Pi^a{}_b$, respectively. Stationarity with respect to the gauge potentials φ^μ and $\psi^a{}_\mu$ yields balance equations for linear and angular momentum. Notably, this summary does not involve a spacetime metric and dispenses with any scalar gravitational potential: gravitational accelerations are carried instead by the time-space components of the connection. No dimensionful constants appear until normalization with physical quantities in sections 7 and 8.

Concept	Definition	Mathematical notation
Gauge potentials	Motion Intrinsic deformation	φ^μ $\psi^a{}_\mu$
Induced geometrical potentials	Velocity-distortion Spin-bend-twist	$\beta^a = \psi^a{}_\mu\, \mathrm{d}\varphi^\mu$ $\kappa^a{}_b = \psi^a{}_\mu\, \mathrm{d}(\psi^{-1})^\mu{}_b$
Field strengths	Intrinsic torsion Intrinsic curvature	$\Sigma^a = \mathrm{d}\beta^a + \kappa^a{}_b \wedge \beta^b$ $\Lambda^a{}_b = \mathrm{d}\kappa^a{}_b + \kappa^a{}_c \wedge \kappa^c{}_b$
Intrinsic Bianchi identities		$\mathscr{D}\Sigma^a = \Lambda^a{}_b \wedge \beta^b$ $\mathscr{D}\Lambda^a{}_b = 0$
Geometrical incompatibilities	Dislocations Disclinations Point defects	$\alpha^a = \psi^a{}_\mu\, \mathrm{d}^2\varphi^\mu$ $\Theta^a{}_b = -(\mathrm{d}^2\psi^a{}_\mu)(\psi^{-1})^\mu{}_b$ $\Pi^a{}_b = (\mathrm{D}\psi^a{}_\mu)(\psi^{-1})^\mu{}_b$
Field equations		$\Sigma^a = \alpha^a$ $\Lambda^a{}_b = \Theta^a{}_b$
Defect Bianchi identities		$\mathscr{D}\alpha^a = \Theta^a{}_b \wedge \beta^b$ $\mathscr{D}\Theta^a{}_b = 0$
Intrinsic Lagrangian capacity		$L = L(\beta^a, \Sigma^a, \Lambda^a{}_b, \Pi^a{}_b)$
Euler–Lagrange (balance) equations	Linear momentum Angular momentum	$\mathscr{D}\sigma_a = (\iota_{e_a}\Sigma^b)\wedge\sigma_b + (\iota_{e_a}\Lambda^b{}_c)\wedge\tau_b{}^c$ $+ (\iota_{e_a}\mathscr{D}\Pi^c{}_d)\wedge\pi_c{}^d - (\iota_{e_a}\Pi^c{}_d)\,\mathscr{D}\pi_c{}^d$ $\mathscr{D}\tau_a{}^b = \sigma_a\wedge\beta^b - \Pi^b{}_c\wedge\pi_a{}^c + \pi_c{}^b\wedge\Pi^c{}_a$

7. Metric-free gravitational waves

In this section, we find plane-wave solutions to the defect-free linearized field equations and calibrate the signal speed with the speed of light.

7.1. Linearized field equations

Gravitational waves arise in this framework as smooth, propagating variations in the intrinsic geometry of spacetime. We expand the motion (2) and intrinsic deformation (4) around a flat, torsion-free, and curvature-free background as

$$\varphi^\mu = \delta^\mu{}_{\mu'} X^{\mu'} + \varepsilon\, s^\mu\left(X^{\mu'}\right), \qquad \psi^a{}_\mu = \delta^a{}_\mu + \varepsilon\, r^a{}_\mu\left(X^{\mu'}\right). \tag{55}$$

From these fields, the velocity-distortion 1-forms (7) become

$$\beta^a = \psi^a{}_\mu\, \mathrm{d}\varphi^\mu = \overline{\beta}^a + \varepsilon\, b^a + O\left(\varepsilon^2\right), \tag{56a}$$

$$b^a \equiv r^a{}_{\mu'}\, \mathrm{d}X^{\mu'} + \mathrm{d}s^a, \qquad s^a \equiv \delta^a{}_\mu\, s^\mu, \tag{56b}$$

where $\overline{\beta}^a = \delta^a{}_{\mu'}\, \mathrm{d}X^{\mu'}$ on the flat background. The perturbation b^a represents the *wave-induced change* in the velocity-distortion.

Similarly, the spin-bend-twist connection (9) expands as

$$\kappa^a{}_b = -\left(\psi^{-1}\right)^\mu{}_b\, \mathrm{d}\psi^a{}_\mu = \varepsilon\, k^a{}_b + O\left(\varepsilon^2\right), \tag{57a}$$

$$k^a{}_b \equiv -\mathrm{d}r^a{}_b, \qquad r^a{}_b \equiv r^a{}_\mu\, \delta^\mu{}_b. \tag{57b}$$

Table 2. Comparison table between the metric-free defect formulation and standard MAG/TEGR frameworks. The rightmost column is included only to provide points of contact; this paper does not assume a fundamental metric.

Concept	Metric-free defect formulation	MAG / TEGR correspondence
Fundamental variables	Coframe β^a and connection $\kappa^a{}_b$ No fundamental metric	MAG: (g,Γ) or $(e^a,\omega^a{}_b,g_{ab})$ TEGR: $(e^a,\omega^a{}_b)$ with sector constraints
Field strengths	$\Sigma^a = \mathrm{d}\beta^a + \kappa^a{}_b \wedge \beta^b$ $\Lambda^a{}_b = \mathrm{d}\kappa^a{}_b + \kappa^a{}_c \wedge \kappa^c{}_b$	Torsion T^a (MAG/TEGR) curvature $R^a{}_b$ (MAG)
Nonmetricity	Not fundamental If $g = \eta_{ab}\beta^a \otimes \beta^b$ is chosen, Q is induced	MAG: $Q_{ab} \equiv -Dg_{ab}$ symmetric TEGR: $T^a = 0$, $R^a{}_b = 0$, $Q \neq 0$
Bianchi identities	$\mathscr{D}\Sigma^a = \Lambda^a{}_b \wedge \beta^b$ $\mathscr{D}\Lambda^a{}_b = 0$	MAG: $DT^a = R^a{}_b \wedge e^b$ MAG: $DR^a{}_b = 0$
Sources	Defect currents $(\alpha^a, \Theta^a{}_b)$ $\Sigma^a = \alpha^a$, $\Lambda^a{}_b = \Theta^a{}_b$	MAG: matter currents (stress/hypermomentum) TEGR: sources in field equations of constrained sector
Interpretation	Mass density from time-space disclinations holonomy/flux observables tied to defects	GR/MAG: mass-energy as external stress-energy TEGR: invariants built from T and/or Q
Action / measure	Capacity-based 4-form measure (no $\sqrt{-g}$) $L(\beta^a, \Sigma^a, \Lambda^a{}_b, \Pi^a{}_b)$ (4-form capacity)	MAG/GR: $\sqrt{-g}\,\mathrm{d}^4x$ (or $e\,\mathrm{d}^4x$) TEGR: scalars built from torsion/nonmetricity in metric-based measure

The perturbation $k^a{}_b$ is the wave-induced change in the spin-bend-twist connection. To first order, the defect-free system field equations (22), $\Sigma^a = 0$ and $\Lambda^a{}_b = 0$, become

$$\mathrm{d}b^a + k^a{}_b \wedge \overline{\beta}^b = 0\,, \tag{58a}$$

$$\mathrm{d}k^a{}_b = 0\,. \tag{58b}$$

7.1.1. Metric comparison

If one temporarily introduces the emergent metric (16) to define the Hodge dual $*$, then the first-order system (58*a*) and (58*b*) implies the second-order wave equations

$$\mathrm{d} * \mathrm{d}b^a = 0\,, \qquad \mathrm{d} * \mathrm{d}k^a{}_b = 0\,. \tag{59}$$

These are similar in form to the linearized gravitational-wave equations of GR, in that they describe massless propagation governed by the same flat-background wave operator. They confirm that, in this linearized source-free regime, both the coframe and connection perturbations propagate as massless waves on the flat background. The introduction of the metric here serves only to exhibit this familiar correspondence and is not required for the metric-free analysis that follows.

7.2. Plane-wave solutions

We now seek monochromatic plane-wave solutions of (58*a*) and (58*b*) of the form

$$b^a = B^a\, \mathrm{e}^{\mathrm{i}k_{\mu'}X^{\mu'}}\,, \qquad k^a{}_b = K^a{}_b\, \mathrm{e}^{\mathrm{i}k_{\mu'}X^{\mu'}}\,, \tag{60}$$

where B^a and $K^a{}_b$ are constant polarization 1-forms and $k = k_{\mu'}\,\mathrm{d}X^{\mu'}$ a constant wave covector. Substitution into the linearized field equations yields

$$\mathrm{i}k \wedge B^a + K^a{}_b \wedge \overline{\beta}^b = 0\,, \tag{61a}$$

$$\mathrm{i}k \wedge K^a{}_b = 0\,. \tag{61b}$$

Since $k\wedge k=0$, this implies that

$$K^a{}_b = C^a{}_b\, k, \tag{62a}$$

$$\mathrm{i}\, B^a + C^a{}_b \overline{\beta}^b = D^a\, k, \tag{62b}$$

for constants $C^a{}_b$ and D^a, thereby constraining amplitudes and polarizations.

7.2.1. Characteristics and signal speed

To determine the propagation speed, we consider the wave covector $k=\omega\overline{\beta}^0-\bar{k}\overline{\beta}^1$ corresponding to a plane wave traveling in the $\bar{e}_1$ direction, where $\omega=\iota_u k$ and $\bar{k}=\iota_{\bar{e}_1}k\geqslant 0$ are its temporal and spatial components. We seek characteristic directions

$$\xi_\pm = \bar{e}_0 \pm s\bar{e}_1 \tag{63}$$

along which the phase $k_{\mu'}X^{\mu'}$ remains constant. Evaluating k on these vectors gives

$$k(\xi_\pm) = \omega \mp s\bar{k} = 0 \quad \Longrightarrow \quad s = \frac{\omega}{\bar{k}}. \tag{64}$$

Hence, monochromatic plane waves propagate at the speed $s=\omega/\bar{k}$, which is frequency-independent and represents the intrinsic conversion factor between temporal and spatial coordinates in the background geometry.

We now identify this conversion factor with the constant c introduced in section 2.1, so that $s=c$. Gravitational waves have been directly observed, and their measured propagation speed agrees with the speed of light in vacuum to high precision (Abbott *et al* 2016, 2017, 2021, 2023). Accordingly, we interpret c as the universal signal speed governing both electromagnetic and gravitational disturbances.

7.2.2. Metric comparison

Equation (64) follows purely from the dual pairing between the covector k and the characteristic vectors $\xi_\pm$. No spacetime metric has been introduced: $s=\omega/\bar{k}$ represents the intrinsic conversion factor between temporal and spatial coordinates in the background dual frames $(\bar{e}_a,\bar{e}^a=\overline{\beta}^a)$. When a metric is reconstructed, the same relation appears as the usual null condition $g^{-1}(k,k)=0$, but here it arises solely from the characteristic geometry of the first-order system.

7.2.3. Transverse and traceless polarizations

The linearized gauge symmetries $\delta b^a=\mathrm{d}\zeta^a+\chi^a{}_b\overline{\beta}^b$ and $\delta k^a{}_b=-\mathrm{d}\chi^a{}_b$ preserve the first-order field equations (58*a*) and (58*b*). For plane-wave phases $\zeta^a=Z^a\,\mathrm{e}^{\mathrm{i}k_{\mu'}X^{\mu'}}$ and $\chi^a{}_b=H^a{}_b\,\mathrm{e}^{\mathrm{i}k_{\mu'}X^{\mu'}}$, the amplitudes transform as $\delta B^a=\mathrm{i}Z^a k+H^a{}_b\overline{\beta}^b$ and $\delta K^a{}_b=-\mathrm{i}H^a{}_b k$. Choosing $Z^a=D^a$ removes the longitudinal components $D^a k$ of B^a, while $H^a{}_b$ eliminates all elements of $C^a{}_b$ carrying a 0 or 1 index. After gauge fixing, only the symmetric, trace-free 2×2 block $C^i{}_j$ in the orbit plane $(i,j=2,3)$ remains, corresponding to the two independent transverse-traceless polarizations $(h_+,h_\times)$.

The designations 'transverse' and 'traceless' are purely algebraic: they refer to the absence of components in the propagation subspace $(0,1)$ and to vanishing internal trace with respect to $\delta^i{}_j$. No metric or inner product is used; the gauge elimination proceeds entirely within the exterior calculus and dual-frame structure. Hence, the two surviving degrees of freedom correspond to intrinsic shear-type excitations of the coframe, not to metric perturbations.

Thus, the framework reproduces the standard gravitational-wave degrees of freedom without invoking a metric, parallel to pre-metric electrodynamics (Hehl and Obukhov 2003, Itin 2009).

7.3. Spacetime defect detection protocol

In this section, we demonstrate that the linearized field equations with geometric defect sources furnish integral relations that connect the intrinsic spacetime geometry with observable, topologically protected quantities[5]. Applying Stokes' theorem yields measurement protocols that distinguish transient gravitational wave phenomena from permanent, defect-induced spacetime deformations. These relations establish a direct operational pathway for detecting and characterizing geometrical spacetime defects.

[5] These quantities are topologically protected in the sense that their values depend only on the global defect content enclosed by the measurement surface, and remain invariant under smooth deformations of the geometric fields away from the core.

7.3.1. Integral formulation

In the presence of defects, the linearized field equations (58*a*) and (58*b*) take the following form:

$$\mathrm{d}b^a + k^a{}_b \wedge \overline{\beta}^b = \alpha^a\,, \tag{65a}$$

$$\mathrm{d}k^a{}_b = \Theta^a{}_b\,. \tag{65b}$$

Applying Stokes' theorem to an oriented 2-surface $S \subset M$ with boundary $\partial S = C$[6], we obtain:

$$\oint_C k^a{}_b = \int_S \Theta^a{}_b\,, \tag{66a}$$

$$\oint_C b^a + \int_S k^a{}_b \wedge \overline{\beta}^b = \int_S \alpha^a\,. \tag{66b}$$

Under infinitesimal coframe rotations $r^a{}_b \mapsto r^a{}_b + \mathrm{d}\varrho^a{}_b$, one has $k^a{}_b \mapsto k^a{}_b - \mathrm{d}^2\varrho^a{}_b = k^a{}_b$ at linear order and for smooth $\varrho^a{}_b$, so the holonomy integrals (66*a*) are gauge-invariant to $O(\varepsilon)$. Similarly, under infinitesimal shifts $s^a \mapsto s^a + \mathrm{d}\varsigma^a$, $b^a \mapsto b^a + \mathrm{d}\varsigma^a$, so $\oint_C b^a$ is unaffected on contractible loops; the second term on the left in (66*b*) accounts for coupling to the background coframe.

In the absence of defects, the circulation integrals around contractible loops vanish. Thus, nontrivial values of $\oint b^a$ or $\oint k^a{}_b$ signal topological obstructions–analogous to crystal dislocations or magnetic flux tubes–that local field redefinitions cannot remove.

7.3.2. Spacetime defects

The integral relations (66*a*) and (66*b*) naturally define spacetime analogs of classical defect characterization from material science. The *spacetime Frank tensor*

$$F^a{}_b \equiv \int_S \Theta^a{}_b \tag{67}$$

quantifies the total spacetime disclination flux piercing the measurement surface S. Notably, the surface S can be chosen as a space-time surface as opposed to a purely spatial surface used in crystallography. It manifests physically as the rotational closure failure, which is directly measurable as the holonomy integral

$$F^a{}_b = \oint_C k^a{}_b \tag{68}$$

around a detector loop $C = \partial S$.

Similarly, the *spacetime Burgers vector*

$$B^a \equiv \int_S \alpha^a \tag{69}$$

encodes the total spacetime dislocation flux through S. This quantity is probed through the translational closure failure represented by the integral of the coframe perturbation

$$B^a = \oint_C b^a + \int_S k^a{}_b \wedge \overline{\beta}^b, \tag{70}$$

where the additional term accounts for coupling between intrinsic deformation and the background coframe.

This framework extends the classical crystallographic analysis of dislocations and disclinations into the domain of spacetime geometry: just as materials scientists characterize defects by circuit integrals of displacement and rotation fields around defect cores, gravitational wave detectors and arrays of test masses can perform analogous holonomy and strain measurements to map the topological defect content in the geometry of spacetime itself.

In this sense, the measurement protocol represents a form of *spacetime crystallography*, where gravitational wave observatories act as instruments for diagnosing the geometric and topological disorder in the gravitational field, potentially revealing new physics beyond smooth perturbative waves.

[6] In what follows, all equalities involving integrals of tensor-valued forms are understood componentwise in the fixed background coframe $\{\overline{\beta}^a\}$, i.e. in the detector-calibrated trivialization used for the linearized protocol.

8. Mass from geometric incompatibility

Motivated by ideas from Katanaev and Volovich (1992) and Katanaev (2005), we define the *geometric mass density* as the time-space disclination component

$$\rho_{\rm geom} \equiv \iota_{e_i}\iota_u \Theta^i{}_0 \,, \tag{71}$$

where the sign fixes the orientation convention used throughout this paper. Using the field equation

$$\Lambda^i{}_0 = \Theta^i{}_0 \,, \tag{72}$$

we may equivalently write

$$\iota_{e_i}\iota_u \Lambda^i{}_0 = \rho_{\rm geom} \,, \tag{73}$$

which we interpret as a *geometrical Poisson equation*.

A time-space disclination, denoted as $\Theta^i{}_0$, is supported on a timelike worldsheet, which has a codimension of 2 (see appendix A.4.3). Although it extends through spacetime, the 'source' (71) on a constant time slice appears pointlike. This is because the mass readout in equation (71) involves two interior products: one along the vector u and another along a spatial direction e_i. These contractions utilize the two tangential directions of the worldsheet, leading to a scalar distribution at the locations where the worldsheet intersects the slice. Therefore, on each spatial slice, the source manifests as a point mass at the puncture(s) in the geometrical Poisson equation (73).

We interpret $\Lambda^i{}_0$ geometrically as illustrated in figure 2. For the infinitesimal rectangular loop spanned by $(\Delta T)\, e_0$ and $(\Delta X^j)\, e_j$, parallel transport of the time basis vector $w = e_0$ along the loop yields the spatial deflection

$$\Delta w^i \approx \Lambda^i{}_{00j}\, (\Delta T)\, \left(\Delta X^j\right) . \tag{74}$$

Thus, $\Lambda^i{}_{00i}$ (no sum over i) is the longitudinal tidal stretch/compression along the i-direction: negative values focus nearby worldlines along i, positive values defocus. The trace $\sum_{i=1}^{3} \Lambda^i{}_{00i} = \Lambda_{00}$, which appears in (71) via the field equation (72), is therefore a divergence-type quantity controlling volumetric focusing of a congruence.

To connect (73) with a physically measured mass density and a Newtonian-type acceleration field on each time slice, we now explicitly introduce the universal conversion constant c identified as the speed of light in section 7. Thus, we define the *gravitational acceleration* components by

$$g^i \equiv c^2\, \iota_u \kappa^i{}_0 \,, \tag{75}$$

so that g^i has the physical dimensions of acceleration. The associated spatial acceleration flux 2-form is

$$\hat{g} \equiv g^i\, \hat{\epsilon}_i \,, \tag{76}$$

where, using (34), $\hat{\epsilon} \equiv \iota_u \epsilon$ is the spatial 3-form capacity and $\hat{\epsilon}_i \equiv \iota_u \epsilon_i$ its 2-form cascade.

We now seek solutions to (73) in the quasi-static, weak-connection limit. To make this relation explicit, we foliate the exterior derivative into temporal and spatial parts (e.g. Choquet-Bruhat *et al* 1982, Frankel 2011):

$$\mathrm{d} = \mathrm{d}T \wedge \mathcal{L}_u + \bar{\mathrm{d}} \,, \tag{77}$$

where $\mathcal{L}_u$ denotes the Lie derivative with respect to the Lagrangian four-velocity u, and where

$$\bar{\mathrm{d}} \equiv \mathrm{d}\big|_{\rm spatial} \tag{78}$$

represents the exterior derivative restricted to spatial directions (i.e. with $\mathrm{d}T = 0$).

Using $\Lambda^i{}_0 = \mathrm{d}\kappa^i{}_0 + \kappa^i{}_a \wedge \kappa^a{}_0$, the capacity identities (33a)–(33c), and neglecting quadratic terms in κ in the quasi-static, weak-connection regime (where $\mathcal{L}_u \simeq 0$, such that Cartan's formula yields $\bar{\mathrm{d}}\iota_u =$

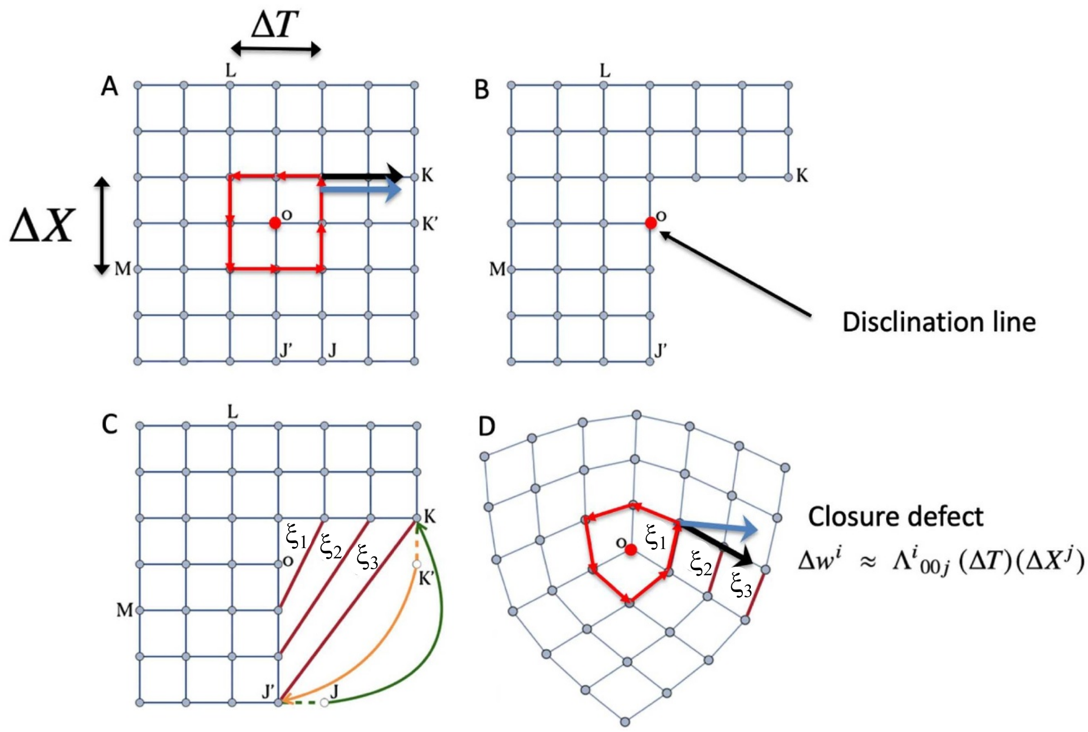

Figure 2. Illustration of a time-space wedge disclination based on the Volterra 'cut-and-weld' protocol. *Top left (A):* a time basis vector $w = e_0$ (black arrow) is parallel transported around the infinitesimal rectangular loop (red) spanned by $(\Delta T)\,e_0$ and $(\Delta X^j)\,e_j$ and returns to the same orientation at the end of the loop (blue arrow). *Top right (B):* a time-space wedge is removed (Volterra 'cut'). *Bottom left (C):* the time and space surfaces of the cut are reattached as shown (Volterra 'weld'). *Bottom right (D):* in the welded timespace, parallel transport of the time vector (black arrow) around the red loop enclosing the disclination line (red dot) results in a vector with a different orientation (blue arrow). The closure defect is the spatial deflection $\Delta w^i \approx \Lambda^i{}_{00j}\,(\Delta T)(\Delta X^j)$.

$-\,\iota_u \bar{\mathrm{d}}$, and the spatial capacities are static so that $\bar{\mathrm{d}}\hat{\epsilon}_i = 0$), the field equation (72) implies the *metric-free Gauss law*:

$$\begin{aligned}
\bar{\mathrm{d}}\hat{g} &= \bar{\mathrm{d}}g^i \wedge \hat{\epsilon}_i + g^i\,\bar{\mathrm{d}}\hat{\epsilon}_i \\
&= c^2\,\bar{\mathrm{d}}\left(\iota_u \kappa^i{}_0\right) \wedge \hat{\epsilon}_i \\
&= -\,c^2\,\iota_u\left(\bar{\mathrm{d}}\kappa^i{}_0\right) \wedge \hat{\epsilon}_i \\
&= -\,c^2\,\left(\iota_u \Lambda^i{}_0\right) \wedge \hat{\epsilon}_i \\
&= -\,c^2\,\left(\iota_{e_i}\iota_u \Lambda^i{}_0\right)\hat{\epsilon} \\
&= -\,c^2\,\rho_{\mathrm{geom}}\,\hat{\epsilon}\,.
\end{aligned} \tag{79}$$

Equation (79) expresses that the divergence of the acceleration flux equals the geometric disclination density.

Integrating (79) over any compact spatial region V gives[7]

$$\int_V \rho_{\mathrm{geom}}\,\hat{\epsilon} = -\frac{1}{c^2}\int_{\partial V}\hat{g}. \tag{80}$$

Consistency with Newton's law of gravitation

$$\int_V \rho\,\hat{\epsilon} = -\frac{1}{4\pi G}\int_{\partial V}\hat{g} \tag{81}$$

requires identifying

$$\boxed{\rho = \frac{c^2}{4\pi G}\,\rho_{\mathrm{geom}}\,.} \tag{82}$$

[7] Appendix A.3 gives a controlled regularization family for defect cores and justifies taking the limit after integrating the smooth Gauss law, yielding the distributional identity used here.

This identification plays the same role as Einstein's alignment of the geometric field equations with Newton's law of gravitation: just as Einstein's formulation determined the factor $8\pi G/c^4$ in front of the Einstein tensor, the Newtonian Gauss law (81) specifies the proportionality constant between geometric disclination density and physical mass density, leading to (82).

The contraction (71) can be carried all the way to the Ricci tensor. From (72) we have

$$\iota_{e_i}\iota_u \Theta^i{}_0 = \Lambda^i{}_{00i}\,, \tag{83}$$

and in regions where $\rho \neq 0$ the intrinsic and full curvatures coincide, so that

$$\Lambda^i{}_{00i} = R^i{}_{00i} = R_{00}\,, \tag{84}$$

where $R_{\mu\nu} = R^\tau{}_{\mu\nu\tau}$ is the Ricci tensor. Thus, the disclination-based definition of mass density (82) coincides exactly with the 00 component of the Ricci tensor that sources gravity in the Newtonian limit of GR.

The interpretation of (82) is direct: a time-space wedge disclination *is* mass density. Unlike Einstein's postulate of a balance between curvature and stress-energy, here matter = geometry follows naturally from incompatibility, similar to the thermodynamic/topological emergence of gravitation (e.g. Jacobson 1995, Padmanabhan 2010, Verlinde 2017). The choice of u selects an observer congruence, just as in relativity, different observers decompose $T_{\mu\nu}$ into densities and fluxes. The invariant content is the disclination itself.

The identification (82) does not in itself enforce $\rho > 0$: the sign depends on the chosen time orientation, the orientation of the spatial coframe, and the sign convention in (75) used to recover Newton's law of gravitation (81). With conventional choices—future-pointing u, a right-handed spatial frame, and $g^i > 0$ for attractive gravity—positive mass density is recovered for ordinary matter. Reversing these conventions yields $\rho < 0$, which formally corresponds to a gravitationally repulsive sector that the framework admits at a purely geometric level.

So far, we have treated disclinations as isolated, line-like incompatibilities. In realistic continua, such idealizations are only limiting cases. Beyond the idealized classification of spacetime defects described in appendix A.4.3, the intrinsic deformation $\psi^a{}_\mu$ can exhibit *distributed* incompatibilities (e.g. Evans and Gariepy 1992, Federer 1996, Ambrosio *et al* 2000). In this context, the expression $(\psi^{-1})^a{}_b\, \mathrm{d}^2\psi^b{}_0$ no longer signifies an isolated defect core; instead, it represents a finite volumetric density of failure within the intrinsic deformation field. In this coarse-grained limit, the contraction $\iota_{e_i}\iota_u\Theta^i{}_0$ defines a mass density field supported on regions (volumes), rather than just along lines; see also appendix A.4. Consequently, time-space disclinations transition from singular topological defects to extended distributions of incompatibility represented by $\psi^a{}_\mu$.

Once matter is formed through such volumetric disclinations ($\rho \neq 0$), the resulting substrate may host additional incompatibilities of the conventional material kind. This suggests a natural conceptual hierarchy: primary spacetime disclinations generate matter, and within that matter, one expects secondary space-space defects—the classical dislocations and disclinations studied by Kondo, deWit, Kröner, and Kleman. While not explicitly required by the field equations, this nested structure of defects within defects offers a unified picture that connects gravitational and material continuum theories.

The identification of mass based on geometrical disclinations avoids treating metric singularities as fundamental, treating mass instead as a smooth geometric failure of integrability localized within the intrinsic deformation field. This concept will play a central role in interpreting the Schwarzschild black hole as a localized geometrical disclination in section 10, where the strength of the disclination is integrated over a defect core to determine the total mass M.

8.1. Metric comparison

Under weak-field conditions, $\iota_{e_i}\iota_u\Lambda^i{}_0 \approx -\partial_i \kappa^i{}_{00}$. If we make the identification

$$\kappa^i{}_{00} \equiv -g^{ij}\,\partial_j\Phi/c^2\,, \tag{85}$$

where Φ is the Newtonian gravitational potential, then

$$\iota_{e_i}\iota_u\Lambda^i{}_0 = \frac{1}{c^2}\,\nabla^2\Phi\,. \tag{86}$$

Thus, based on the identification (82), the geometrical Poisson equation (73) then becomes the classical Poisson equation

$$\nabla^2\Phi = 4\pi G\rho. \tag{87}$$

9. Gravitational Lagrangian

In this section, we first recall the classical MAG Lagrangian before constructing a minimal metric-free gravitational Lagrangian based on the discussion of the Lagrangian volume capacity in section 3.

9.1. Metric comparison: MAG Lagrangian

Metric-affine gravitation theory generalizes Einstein's approach by treating the metric and connection as independent variables, allowing for torsion and nonmetricity. The geometry Lagrangian of metric-affine gravitation theory (e.g. Trautman 1973, Dudek and Garecki 2019, Montesinos *et al* 2020) is

$$\begin{aligned} L_{\mathrm{MAG}} &= \tfrac{1}{4} g^{\sigma\beta}\, \epsilon_{\mu\nu\sigma\tau}\, e^{\mu} \wedge e^{\nu} \wedge R_{\beta}{}^{\tau} \\ &= \tfrac{1}{2}\, \epsilon_{\sigma\tau} \wedge R^{\sigma\tau}\,, \end{aligned} \tag{88}$$

where $R^{\mu}{}_{\nu}$ is the curvature,

$$\epsilon_{\mu\nu\sigma\tau} = \sqrt{-g}\,\varepsilon_{\mu\nu\sigma\tau} \tag{89}$$

is the volume 4-form, and

$$\epsilon_{\sigma\tau} = \tfrac{1}{2!}\sqrt{-g}\,\varepsilon_{\mu\nu\sigma\tau}\, e^{\mu} \wedge e^{\nu} \tag{90}$$

the area 2-form. Here $R^{\sigma\tau} \equiv g^{\tau\beta} R^{\sigma}{}_{\beta}$. The factor $\sqrt{-g}$ is included to render the volume quantities tensorial. MAG reduces to Einstein gravity when one imposes metric compatibility ($\mathrm{D}g_{\mu\nu} = 0$) and zero torsion ($T^{\mu} = 0$).

The variation of the MAG Lagrangian (88) with respect to the fundamental variables yields

$$\frac{\delta L_{\mathrm{MAG}}}{\delta g^{\mu\nu}} = \tfrac{1}{4}\left(\delta^{\sigma}{}_{\mu}\,\delta^{\beta}{}_{\nu} + \delta^{\sigma}{}_{\nu}\,\delta^{\beta}{}_{\mu} - g^{\sigma\beta} g_{\mu\nu}\right) \epsilon_{\sigma\tau} \wedge R_{\beta}{}^{\tau}\,, \tag{91a}$$

$$\frac{\delta L_{\mathrm{MAG}}}{\delta e^{\mu}} = \tfrac{1}{2}\, \epsilon_{\mu\sigma\tau} \wedge R^{\sigma\tau}\,, \tag{91b}$$

$$\frac{\delta L_{\mathrm{MAG}}}{\delta \Gamma^{\mu}{}_{\nu}} = -\tfrac{1}{2}\, \mathrm{D}\epsilon_{\mu}{}^{\nu}\,. \tag{91c}$$

In the presence of matter, these geometric field equations would be sourced by the metrical energy-momentum tensor $\sigma^{\mu\nu}$, canonical energy-momentum current ς_{μ}, and hypermomentum current $\Delta_{\mu}{}^{\nu}$, respectively.

9.2. Metric-free Lagrangian

Let $u^{a} \equiv \iota_u \beta^{a}$ satisfy $\iota_u \mathrm{d}T = 1$. Motivated by the MAG Lagrangian (88), the metric-free Lagrangian 4-form capacity is defined as

$$L \equiv -\mu\, u^{a} u^{b}\, \epsilon_{cb} \wedge \Lambda^{c}{}_{a} + (\iota_u \mathrm{d}T - 1)\,\lambda\,, \tag{92}$$

with constant μ to be fixed below and the capacity-valued area 2-form ϵ_{cb} defined by (32*b*); the 2-form capacity ϵ_{cb} depends only on (β^{a}, ψ) and requires no metric. The constant 4-form capacity λ is the Lagrange multiplier enforcing $\iota_u \mathrm{d}T = 1$.

We vary β^{a}, $\Lambda^{a}{}_{b}$, u, and λ, with the dependent relation $u^{a} \equiv \iota_u \beta^{a}$ so that $\delta u^{a} = \iota_u \delta\beta^{a} + \iota_{\delta u}\beta^{a}$. We treat $\Lambda^{a}{}_{b}$ as the intrinsic curvature 2-form and do not vary the non-tensorial connection $\kappa^{a}{}_{b}$ directly[8]. These variations are used to compute the constitutive stress and couple-stress currents generated by L; the governing Euler–Lagrange equations are the balance equations (50*a*) and (50*b*) obtained from stationarity with respect to φ^{μ} and $\psi^{a}{}_{\mu}$.

The action is

$$S = \int_M L\,, \tag{93}$$

with L given by (92). If defect cores are idealized distributionally, the action and its variation are understood in the regularized current-limit sense described in section 4 and appendix A.3. We have the following contributions.

[8] This is analogous to the Palatini method: curvature 2-forms are varied independently of connections, ensuring tensorial variations (e.g. Hehl *et al* 1995).

λ-variation.

$$\delta_\lambda S = \int_M (\iota_u \mathrm{d}T - 1)\, \delta\lambda \qquad \Longrightarrow \qquad \iota_u \mathrm{d}T = 1\,. \tag{94}$$

Λ-variation. Since L is linear in $\Lambda^c{}_a$,

$$\frac{\partial L}{\partial \Lambda^a{}_b} = -\,\mu\, u^b u^c\, \epsilon_{ac}\,, \tag{95}$$

which yields the couple stress 3-form capacities

$$\tau_a{}^b = \mathscr{D}\left(\frac{\partial L}{\partial \Lambda^a{}_b}\right) = -\,\mu\,\mathscr{D}\left(u^b u^c\, \epsilon_{ac}\right)\,. \tag{96}$$

u-variation. Holding β^a fixed in this step ($\delta\beta^a = 0$) so that $\delta u^a = \iota_{\delta u}\beta^a \equiv \xi^a$, one finds

$$\delta_u S = -\int_M \mu\, \left(\xi^a u^b + u^a \xi^b\right) \epsilon_{cb} \wedge \Lambda^c{}_a + \int_M (\iota_{\delta u}\mathrm{d}T)\, \lambda\,. \tag{97}$$

Since $\iota_{\delta u}\mathrm{d}T = (\mathrm{d}T)_a\, \xi^a$, the u-equations are

$$-\,\mu\, \left(u^b\, \epsilon_{cb} \wedge \Lambda^c{}_a + u^b\, \epsilon_{ca} \wedge \Lambda^c{}_b\right) + (\iota_{e_a}\mathrm{d}T)\, \lambda = 0\,, \tag{98}$$

one equation for each intrinsic index a.

β-variation. We hold u fixed in this step ($\delta u = 0$), so that $\delta u^a = \iota_u\, \delta\beta^a$ and

$$\delta\epsilon_{ab} = \epsilon_{abcd}\, \delta\beta^c \wedge \beta^d\,. \tag{99}$$

Using $(\iota_u\, \delta\beta^a)\, \Omega = \delta\beta^a \wedge \iota_u \Omega$ for 4-forms Ω, and collecting the $\delta\beta^a$ terms, the stress 3-form capacities are

$$\sigma_a = -\,\mu\, u^b \left[u^c\, (\iota_{e_a}\epsilon_{dc}) \wedge \Lambda^d{}_b + (\iota_u \epsilon_{db}) \wedge \Lambda^d{}_a - \epsilon_{db} \wedge \iota_u \Lambda^d{}_a + (\iota_u \epsilon_{da}) \wedge \Lambda^d{}_b - \epsilon_{da} \wedge \iota_u \Lambda^d{}_b\right]\,. \tag{100}$$

9.2.1. Observer-adapted frame

Next, we choose a frame adapted to the congruence so that $\{u^a\} = \{1, 0, 0, 0\}$ and align $\mathrm{d}T$ with the time direction ($\iota_{e_a}\mathrm{d}T = \delta^0{}_a$). Then the u-equations (98) reduce to

$$\lambda = 2\,\mu\, \epsilon_{i0} \wedge \Lambda^i{}_0 = -\,2\,\mu\, \rho_{\mathrm{geom}}\, \epsilon\,, \qquad \epsilon_{j0} \wedge \Lambda^j{}_i + \epsilon_{ji} \wedge \Lambda^j{}_0 = 0\,. \tag{101}$$

The first equation determines λ in terms of the geometric mass density, $\rho_{\mathrm{geom}} = \iota_{e_i}\iota_u \Lambda^i{}_0$, while the second encodes the on-shell compatibility between time-space and purely spatial curvature components.

The components of the stress (100) become

$$\sigma_0 = 2\,\mu\, \epsilon_{i0} \wedge \iota_u \Lambda^i{}_0 = 2\,\mu\, \rho_{\mathrm{geom}}\, \hat{\epsilon}\,, \tag{102a}$$

$$\sigma_i = \mu\, \left(\epsilon_{j0} \wedge \iota_u \Lambda^j{}_i - \epsilon_{i0} \wedge \iota_u \Lambda^0{}_0 - \epsilon_{ij} \wedge \iota_u \Lambda^j{}_0\right)\,, \tag{102b}$$

where $\hat{\epsilon} = \iota_u \epsilon$ denotes the 3D volume capacity.

Identifying $\sigma_0 = \rho c^2\, \hat{\epsilon}$ and recalling $\rho_{\mathrm{geom}} = (4\pi\, G/c^2)\, \rho$ from (82) yields

$$\rho\, c^2 = 2\,\mu\, \rho_{\mathrm{geom}} \qquad \Longrightarrow \qquad \boxed{\mu = \frac{c^4}{8\pi\, G}\,.} \tag{103}$$

The nonzero couple stresses are

$$\tau_i{}^0 = -\,\mu\, \left(\epsilon_{i0j} \wedge \Sigma^j - Q \wedge \epsilon_{i0}\right)\,. \tag{104}$$

where $Q = \mathrm{d}\log\psi$. In the absence of torsion and point defects, the couple stresses vanish.

Finally, these stress and couple-stress 3-form capacities enter the Euler–Lagrange (balance) equations (50*a*) and (50*b*), which govern their covariant conservation in the presence of torsion, curvature, and point defects.

9.3. Summary

The metric-free gravitational Lagrangian capacity (92) encodes the complete energetic content of spacetime geometry. Its variation yields stress and couple-stress current densities, which we interpret physically as rest-energy density, momentum fluxes, and gravitational stresses.

By enforcing the constraint $\iota_u \mathrm{d}T = 1$ with an energetically inert multiplier, the normalization condition (103) is uniquely fixed through the geometric identification of mass density with time-space disclinations.

As a result, all aspects of gravitational energy—including mass, stresses, and their balance equations—emerge directly from geometry, without introducing a separate matter Lagrangian. The only universal constants involved are c, the time-space conversion factor, and G, the coupling of disclinations to mass density.

9.4. Generalizations

The gravitational Lagrangian capacity described in equation (92) is the simplest diffeomorphism- and bundle-covariant 4-form that is linear in curvature. It specifically isolates the time-space sector and reproduces the stress formulas of GR. Similar to GR, where one might consider $f(R)$ or higher-curvature terms (e.g. Capozziello *et al* 2008, Sotiriou and Faraoni 2010), our framework allows for natural generalizations while maintaining a metric-free approach.

Noting that

$$u^a u^b \epsilon_{cb} \wedge \Lambda^c{}_a = \Lambda\,\epsilon\,, \qquad \Lambda \equiv u^a u^b \Lambda^c{}_{acb}\,, \tag{105}$$

(where the equality follows from the algebra of interior products with ϵ and the Kronecker $\delta^a{}_b$ only), a broad class of gravitational Lagrangians is then

$$L = \epsilon f(\Lambda) + (\iota_u \mathrm{d}T - 1)\,\lambda\,, \tag{106}$$

with $f(\Lambda) = -\mu\Lambda + O(\Lambda^2)$ so that the linear limit reproduces (92).

Other admissible metric-free invariants can be constructed by using u^a and ϵ_{ab} to create additional wedge contractions with Σ^a or $\Lambda^a{}_b$, as long as the result is a 4-form capacity. We will leave a systematic classification and exploration of these terms for future work.

Thus, equation (92) serves as an 'Einstein–Hilbert' baseline in a metric-free setting. Moreover, equation (106) demonstrates that this framework can be naturally generalized, similar to $f(R)$ extensions of GR (e.g. Sotiriou and Faraoni 2010, Capozziello and Laurentis 2011, Järv *et al* 2018, Baldazzi *et al* 2022), while maintaining its core geometric interpretation.

10. Black holes

In this theory, a black hole is interpreted as a *localized geometrical defect* rather than a singularity of the spacetime metric. In the vacuum exterior $U = M \setminus C$ of the defect core C, the intrinsic field equations (10*a*) and (10*b*) reduce to

$$\Sigma^a = 0\,, \qquad \Lambda^a{}_b = 0\,, \tag{107}$$

ensuring that all intrinsic curvature and torsion are distributionally supported on C.

On U, the *full* coframe torsion and curvature, T^a and $R^a{}_b$, are determined by (25). These are the complete geometric field expressions: the intrinsic part vanishes in U, while the smooth connection (15), $\Omega^a{}_b$, generates the nontrivial exterior curvature profile.

In this section, we focus on an exterior branch that is comparable to GR. This branch is defined on the region U with the following conditions: intrinsic vacuum $\Sigma^a = 0$, $\Lambda^a{}_b = 0$, $\Pi^a{}_b = 0$, and a torsionless full connection where $T^a = 0$. For comparison purposes, we also limit our considerations to the metric-compatible (Lorentz-reduced) sector, where $q_{ab} = 0$.

The complete metric-free theory, including its variables and identities, is summarized in table 1. Here, we specifically concentrate on the exterior branch that directly interfaces with the standard GR black hole sector.

The Lorentz reduction is achieved by choosing a fixed internal bilinear form g_{ab} of Lorentz signature on U (i.e. $\mathrm{d}g_{ab} = 0$, so g_{ab} is non-dynamical) and imposing vanishing nonmetricity $q_{ab} \equiv -\mathrm{D}g_{ab} = 0$. Equivalently, $\kappa_{ab} + \kappa_{ba} = 0$ with $\kappa_{ab} \equiv g_{ac}\kappa^c{}_b$, so $\kappa^a{}_b$ is a spin (Lorentz) connection. Without loss of generality, one may take $g_{ab} = \eta_{ab}$ in an orthonormal internal frame.

This approach establishes compatibility: the kinematics derived from defect theory permit exterior profiles that reproduce the standard GR black hole geometries outside a compact defect core.

10.1. Spherical coframe

For spherical orbits, we introduce an oriented coframe $(\vartheta^2, \vartheta^3)$ and a connection γ obeying the Cartan system

$$\mathrm{d}\vartheta^2 + \gamma \wedge \vartheta^3 = 0\,, \qquad \mathrm{d}\vartheta^3 - \gamma \wedge \vartheta^2 = 0\,, \qquad \mathrm{d}\gamma = \vartheta^2 \wedge \vartheta^3\,, \tag{108}$$

with topological normalization

$$\frac{1}{4\pi}\int_{S^2} \mathrm{d}\gamma = 1\,. \tag{109}$$

This fixes the orientation and the 4π-flux of the orbit curvature, serving as a metric-free stand-in for the area of a unit sphere.

By spherical symmetry, the two orbit directions are equivalent up to rotation. Hence, the intrinsic coframe restricted to the S^2 orbits must be proportional to a fixed, normalized orbit coframe $(\vartheta^2, \vartheta^3)$ satisfying the Cartan system (108). Thus, stationarity and SO(3) symmetry fix the velocity-distortion coframe:

$$\beta^0 = A(R)\,\mathrm{d}T\,, \qquad \beta^1 = B(R)\,\mathrm{d}R\,, \qquad \beta^2 = C(R)\,\vartheta^2\,, \qquad \beta^3 = C(R)\,\vartheta^3\,, \tag{110}$$

with $A, B, C > 0$ on U, and where $C(R)$ is an orbit scale factor that depends only on the radial label R.

The associated *orbit area* 2-capacity is

$$\sigma \;\equiv\; \beta^2 \wedge \beta^3 = C^2(R)\,\vartheta^2 \wedge \vartheta^3 = C^2(R)\,\mathrm{d}\gamma\,. \tag{111}$$

Integrating σ over the 2-sphere of constant radial label R, denoted $S^2(R)$, using (109), gives

$$\frac{1}{4\pi}\int_{S^2(R)} \sigma = \frac{1}{4\pi}\int_{S^2(R)} C^2(R)\,\mathrm{d}\gamma = C^2(R)\,. \tag{112}$$

This relation shows that $C(R)$ plays the role of an *intrinsic radius* assigned to each spherical orbit: its square equals the normalized flux of the orbit area.

In the *areal gauge*, one simply sets

$$C(R) = R\,, \qquad \text{so that} \qquad \frac{1}{4\pi}\int_{S^2(R)} \beta^2 \wedge \beta^3 = R^2\,. \tag{113}$$

10.2. GR-compatible, torsionless exterior and curvature

On U we impose the torsionless condition on the full coframe connection (23),

$$T^a = \mathrm{d}\beta^a + \Gamma^a{}_b \wedge \beta^b = 0\,. \tag{114}$$

At this stage $\Gamma^a{}_b$ is a general connection 1-form, and no symmetry (or reduction) of the internal indices is assumed.

To extract an exterior branch directly comparable with the torsionless vacuum solutions of GR, we now *restrict* to the metric-compatible (Lorentz-reduced) sector on U. Concretely, we choose a fixed internal bilinear form g_{ab} of Lorentz signature on U (so $\mathrm{d}g_{ab} = 0$), and we impose vanishing intrinsic nonmetricity (19),

$$q_{ab} \equiv -\mathrm{D}g_{ab} = 0 \qquad \text{on } U. \tag{115}$$

With $\Gamma_{ab} \equiv g_{ac}\Gamma^c{}_b$ and g_{ab} fixed, condition (115) is equivalent to

$$\Gamma_{ab} = -\Gamma_{ba}\,, \tag{116}$$

so that $\Gamma^a{}_b$ is a metric-compatible (spin) connection relative to g_{ab}.

This step is not a gauge choice: it is a sector restriction that removes the nonmetricity degrees of freedom in the exterior. More general torsionless exteriors with $q_{ab} \neq 0$ (and/or additional point-defect content) are allowed in the full theory, but are not pursued here because our purpose in this section is to establish compatibility with the standard GR black-hole exteriors outside a compact defect core.

Thus, we find

$$\Gamma^0{}_1 = D\,\beta^0\,, \qquad \Gamma^2{}_1 = E\,\beta^2\,, \qquad \Gamma^3{}_1 = E\,\beta^3\,, \qquad \Gamma^2{}_3 = \gamma\,, \tag{117}$$

with

$$D \equiv \frac{A'}{AB}, \tag{118}$$

and

$$E \equiv \frac{C'}{BC}. \tag{119}$$

Up to antisymmetry, these are the only independent, nonvanishing components that are compatible with stationarity, spherical symmetry, and the torsionless condition. The remaining entries are either fixed by antisymmetry or vanish.

Because we are in the metric-compatible sector (116), the curvature 2-forms satisfy $R^a{}_b = -R^b{}_a$ and, under spherical symmetry, a single curvature scalar $K(R)$ controlling all full curvature components (24):

$$\begin{aligned} &R^0{}_1 = 2K\beta^0 \wedge \beta^1, && R^0{}_2 = K\beta^0 \wedge \beta^2, && R^0{}_3 = K\beta^0 \wedge \beta^3, \\ &R^1{}_2 = K\beta^1 \wedge \beta^2, && R^1{}_3 = K\beta^1 \wedge \beta^3, && R^2{}_3 = 2K\beta^2 \wedge \beta^3. \end{aligned} \tag{120}$$

Using (24), $R^a{}_b = \mathrm{d}\Gamma^a{}_b + \Gamma^a{}_c \wedge \Gamma^c{}_b$, and (116), we find

$$\begin{aligned} &R^0{}_1 = -\left(\frac{D'}{B} + D^2\right)\beta^0 \wedge \beta^1, && R^0{}_2 = -DE\beta^0 \wedge \beta^2, && R^0{}_3 = -DE\beta^0 \wedge \beta^3, \\ &R^1{}_2 = -\left(\frac{E'}{B} + E^2\right)\beta^1 \wedge \beta^2, && R^1{}_3 = -\left(\frac{E'}{B} + E^2\right)\beta^1 \wedge \beta^3, && R^2{}_3 = \left(\frac{1}{C^2} - E^2\right)\beta^2 \wedge \beta^3, \end{aligned} \tag{121}$$

with $R^a{}_b = -R^b{}_a$.

Comparing (120) with (121) gives the identities

$$K = -DE = -\left(\frac{E'}{B} + E^2\right), \tag{122a}$$

$$2K = -\left(\frac{D'}{B} + D^2\right) = \frac{1}{C^2} - E^2. \tag{122b}$$

The Bianchi identity $\mathrm{D}R^a{}_b = 0$ then yields

$$\frac{1}{B}\frac{\mathrm{d}K}{\mathrm{d}R} + 3\frac{C'}{BC}K = 0 \qquad \Longrightarrow \qquad K(R) = \frac{\kappa_0}{C^3(R)}, \tag{123}$$

with an integration constant κ_0.

10.3. Exterior profile

Adopting the areal gauge $C(R) = R$ implies according to (119) and (123) that $E = 1/(BR)$ and $K = \kappa_0/R^3$, so that (122a) gives

$$B^2(R) = \frac{1}{1 - \frac{2\kappa_0}{R}}. \tag{124}$$

Using (118) with this B^2 yields

$$\frac{\mathrm{d}}{\mathrm{d}R}\log A = -\frac{\kappa_0}{R^2\left(1 - \frac{2\kappa_0}{R}\right)}. \tag{125}$$

Integrating and fixing asymptotics $A \to 1$ as $R \to \infty$ yields

$$A^2(R) = 1 - \frac{2\kappa_0}{R}, \qquad B(R) = \frac{1}{A(R)}. \tag{126}$$

The functions $A(R)$ and $B(R) = 1/A(R)$ thus determine the complete torsionless, spherically symmetric coframe (110) in the exterior region. The integration constant κ_0 will be related to the physical mass by the normalization condition in (130).

10.4. Defect charge and mass normalization

The integration constant κ_0 represents the defect charge, geometrically equivalent to the enclosed disclination flux. Because $\Lambda^a{}_b = 0$ on U, the time-space disclination is supported on C. Using (120) we have

$$\iota_u \iota_{e_i} R^i{}_0 = 4K. \tag{127}$$

Let t_ε be a small tubular neighborhood of C, with boundary S^2_ε homologous to the orbits. Then

$$\int_{U \setminus t_\varepsilon} \iota_u \iota_{e_i} R^i{}_0 \,\hat{\epsilon} = 4 \int_{U \setminus t_\varepsilon} K \hat{\epsilon} \xrightarrow{\varepsilon \to 0} -4\pi \kappa_0 , \tag{128}$$

where $\hat{\epsilon} \equiv \iota_u \epsilon$ is the 3D volume capacity (34) and the sign follows from the outward-normal orientation on S^2_ε.

To compare with the mass identification, on a spatial slice, let $V \subset U$ be any compact spatial region whose boundary links the core (i.e. ∂V is homologous to the small sphere S^2_ε in U), and choose ε small enough that $t_\varepsilon \subset V$. Then, the mass identification (82) yields

$$Mc^2 = \int_V \rho c^2 \,\hat{\epsilon} = \frac{c^4}{4\pi G} \int_V \rho_{\mathrm{geom}} \,\hat{\epsilon} = \frac{c^4}{4\pi G} \int_V \iota_{e_i} \iota_u \Theta^i{}_0 \,\hat{\epsilon} = \frac{c^4}{4\pi G} \lim_{\varepsilon \to 0} \int_{V \setminus t_\varepsilon} \iota_{e_i} \iota_u \Theta^i{}_0 \,\hat{\epsilon} , \tag{129}$$

and using $\Lambda^i{}_0 = \Theta^i{}_0$ distributionally on C together with $\iota_u \iota_{e_i} = -\iota_{e_i} \iota_u$, (128) gives

$$Mc^2 = \frac{c^4}{4\pi G} (4\pi \kappa_0) \qquad \Longrightarrow \qquad \kappa_0 = \frac{GM}{c^2} . \tag{130}$$

This matches the mass normalization obtained earlier from the Lagrangian analysis, ensuring consistency across the Newtonian, variational, and black hole regimes.

10.5. Schwarzschild exterior

Substituting (130) into (126) gives the standard profile

$$A^2 (R) = 1 - \frac{2GM}{c^2 R} , \qquad B(R) = \frac{1}{\sqrt{1 - \frac{2GM}{c^2 R}}} , \tag{131}$$

so the exterior coframe is

$$\beta^0 = \sqrt{1 - \frac{2GM}{c^2 R}} \,\mathrm{d}T , \qquad \beta^1 = \frac{1}{\sqrt{1 - \frac{2GM}{c^2 R}}} \,\mathrm{d}R , \qquad \beta^2 = R \vartheta^2 , \qquad \beta^3 = R \vartheta^3 . \tag{132}$$

No spacetime metric field or Hodge dual is required for the exterior coframe derivation; the only additional structure used is the exterior restriction to a metric-compatible connection sector relative to a fixed internal bilinear form g_{ab} (116).

10.5.1. Line element

When a metric is reconstructed from the coframe according to (16), then the line element becomes

$$\mathrm{d}s^2 = -\left(1 - \frac{2GM}{c^2 R}\right) c^2 \mathrm{d}T^2 + \left(1 - \frac{2GM}{c^2 R}\right)^{-1} \mathrm{d}R^2 + R^2 \,\mathrm{d}\Omega^2 , \tag{133}$$

revealing the standard Schwarzschild form, where $\mathrm{d}\Omega^2$ is the metric on the two-sphere.

10.6. Kottler (Schwarzschild-de Sitter) exterior

Allowing a constant isotropic background curvature $K \mapsto K + \Lambda_{\mathrm{cos}}/3$, compatible with the spherical Cartan system (108) and with the Bianchi identity, produces the Kottler exterior with

$$A^2 (R) = 1 - \frac{2GM}{c^2 R} - \frac{\Lambda_{\mathrm{cos}}}{3} R^2 , \qquad B(R) = \frac{1}{A(R)} . \tag{134}$$

In contrast to Einstein gravity, where Λ_{cos} enters through an explicit modification of the field equations, here it appears as an admissible constant-curvature contribution to the *full* exterior curvature compatible with the spherical Cartan system (108) and the Bianchi identity. In the metric comparison, this branch corresponds to the Schwarzschild–de Sitter (Kottler) family.

10.7. Horizon, area, and surface gravity

Horizon as coframe degeneracy. In the torsionless, stationary, spherically symmetric exterior (110)–(126), the temporal coframe component is $\beta^0 = A(R)\,\mathrm{d}T$ with $A(R) \to 1$ as $R \to \infty$. We define the (outer) horizon radius R_{H} intrinsically as the distinguished orbit where the temporal 1-capacity degenerates,

$$A(R_{\mathrm{H}}) = 0\,, \qquad A(R) > 0 \quad \text{for} \quad R > R_{\mathrm{H}}\,. \tag{135}$$

For the Schwarzschild branch (126) this gives $R_{\mathrm{H}} = 2\kappa_0$, i.e. $R_{\mathrm{H}} = 2GM/c^2$ via (130).
Horizon area from 2-capacity flux. The orbit area 2-capacity is $\sigma = \beta^2 \wedge \beta^3$, so by (112) the area of any orbit $S^2(R)$ is determined purely by its flux:

$$\mathrm{Area}\left(S^2(R)\right) \;\equiv\; \int_{S^2(R)} \sigma \;=\; 4\pi C^2(R)\,. \tag{136}$$

In the areal gauge $C(R) = R$, the horizon area is therefore

$$\mathrm{Area}_{\mathrm{H}} = \int_{S^2(R_{\mathrm{H}})} \sigma = 4\pi R_{\mathrm{H}}^2 = 4\pi \left(\frac{2GM}{c^2}\right)^2, \tag{137}$$

obtained without introducing an independent spacetime metric field, a Hodge dual, or any index raising/lowering on spacetime forms (beyond the exterior choice of a fixed internal bilinear form g_{ab} used to select the metric-compatible sector).

Surface gravity from the torsionless connection. Let u denote the stationary observer congruence defined by the intrinsic coframe duality conditions

$$\iota_u \beta^0 = 1\,, \qquad \iota_u \beta^i = 0 \quad (i = 1,2,3)\,. \tag{138}$$

In the torsionless, metric-compatible sector (116) the only time-radial connection component is ${\Gamma^0}_1 = D\beta^0$ with $D = A'/(AB)$ from (118). The frame-covariant 1-form encoding the radial acceleration of the stationary congruence is then

$$a_R \;\equiv\; \iota_u {\Gamma^0}_1 = D\,, \qquad a \;\equiv\; a_R\,\beta^1 = D\beta^1\,. \tag{139}$$

So that the physically normalized acceleration scale is $c^2 D$.

The surface gravity is defined (in the standard geometric way for static horizons) as the redshifted acceleration required to hold station at fixed R, taking the horizon limit:

$$\kappa_{\mathrm{sg}} \;\equiv\; c^2 \lim_{R\to R_{\mathrm{H}}} A(R)\,D(R) \;=\; c^2 \lim_{R\to R_{\mathrm{H}}} \frac{A'(R)}{B(R)}\,, \tag{140}$$

where we used $AD = A'/B$ from (118). This definition is intrinsic to the coframe/connection data and uses only the asymptotic normalization $A \to 1$ (fixing the time scale at infinity).

Schwarzschild value. For the Schwarzschild branch $B = 1/A$ and $A^2 = 1 - 2\kappa_0/R$, so $AD = AA' = \frac{1}{2}\,\mathrm{d}(A^2)/\mathrm{d}R = \kappa_0/R^2$. Evaluating at $R_{\mathrm{H}} = 2\kappa_0$ gives

$$\kappa_{\mathrm{sg}} = c^2\,\frac{\kappa_0}{R_{\mathrm{H}}^2} = \frac{c^4}{4GM}\,, \tag{141}$$

in agreement with the standard Schwarzschild surface gravity.

Kottler value. For the Kottler branch $A^2(R) = 1 - \frac{2GM}{c^2 R} - \frac{\Lambda_{\cos}}{3}R^2$ and $B = 1/A$, so (140) yields

$$\kappa_{\mathrm{sg}} = \frac{c^2}{2}\left|\left(A^2\right)'(R_{\mathrm{H}})\right| = \left|\frac{GM}{R_{\mathrm{H}}^2} - \frac{c^2\Lambda_{\cos}}{3}R_{\mathrm{H}}\right|, \tag{142}$$

where the absolute value accounts for the fact that the same formula applies to either the black-hole horizon or the cosmological horizon. Here R_{H} denotes any positive root of $A^2(R) = 0$ (black-hole or cosmological horizon), and (142) applies at that root.

Metric comparison. If one reconstructs a metric using (16), then (137) and (140) simplify to the standard metric expressions for horizon area and surface gravity in static, spherically symmetric spacetimes. This confirms that the intrinsic coframe and connection diagnostics recover the conventional black hole observables.

10.8. FLRW cosmology

We briefly indicate how a homogeneous and isotropic (spatially flat) reduction is encoded in the coframe-connection variables, in the same GR-compatible sector used for the exterior black-hole profiles. Let $(X^I) = (T, X^1, X^2, X^3)$ be Lagrangian coordinates adapted to a comoving observer congruence u with $\iota_u \mathrm{d}T = 1$. Choose a coframe of the form

$$\beta^0 = \mathrm{d}T\,, \qquad \beta^i = a(T)\,E^i{}_I\,\mathrm{d}X^I\,, \qquad i = 1,2,3\,, \tag{143}$$

where $a(T)$ is the scale factor and $E^i{}_I$ is a constant spatial frame map with $E^i{}_0 = 0$. For the simplest chart-aligned choice one may take $E^i{}_J = \delta^i{}_J$.

As in section 10.2 we impose torsionlessness for the full coframe connection,

$$T^a \equiv \mathrm{d}\beta^a + \Gamma^a{}_b \wedge \beta^b = 0\,, \tag{144}$$

and work in the GR-compatible, metric-compatible sector by choosing the internal bilinear form g_{ab}, as in (16), and imposing $q_{ab} \equiv -\mathrm{D}g_{ab} = 0$. Defining $H(T) \equiv \dot{a}/a$, the spatially flat branch satisfies

$$\mathrm{d}\beta^i = H\,\beta^0 \wedge \beta^i\,. \tag{145}$$

A homogeneous/isotropic torsionless solution is obtained with the connection ansatz

$$\Gamma^i{}_0 = H\beta^i\,, \qquad \Gamma^0{}_i = H\beta^i\,, \qquad \Gamma^i{}_j = 0\,, \tag{146}$$

which yields $T^i = 0$ and $T^0 = 0$.

The full curvature 2-forms are computed as

$$R^a{}_b \equiv \mathrm{d}\Gamma^a{}_b + \Gamma^a{}_c \wedge \Gamma^c{}_b\,, \tag{147}$$

so that

$$R^i{}_0 = (\dot{H} + H^2)\,\beta^0 \wedge \beta^i\,, \tag{148a}$$

$$R^i{}_j = H^2\,\beta^i \wedge \beta^j\,. \tag{148b}$$

If one reconstructs a spacetime metric from the coframe via (16), these map to the usual FLRW curvature scalars in an orthonormal coframe.

In the defect-free exterior away from cores, the intrinsic strengths satisfy $\Sigma^a = 0$ and $\Lambda^a{}_b = 0$ by construction; this does not imply that the exterior spacetime curvature $R^a{}_b$ vanishes, and in particular it does not force H to vanish. Rather, whether $H(T)$ must be trivial is a question of the specific field equations and source content adopted for the exterior branch. In the strictly source-free reduction used for the vacuum black-hole exteriors, the homogeneous/isotropic ansatz typically collapses to $H \equiv 0$; genuine cosmological evolution then requires either (i) nontrivial (defect) source content in the effective exterior equations, or (ii) a controlled extension of the system's capacity beyond the strictly source-free sector.

For instance, by defining a homogeneous effective time-space disclination contraction as $\rho_{\mathrm{geom}}(T) \equiv \iota_{e_i}\iota_u \Theta^i{}_0$, and substituting the FLRW ansatz into the (suitably sourced) field equations (or into a type of $f(\Lambda)$ extension), one can derive an evolution equation for $a(T)$. This equation is driven by the spatially averaged defect content, and when applying the metric-comparison interface, it maps to the standard Friedmann equations.

11. Autoparallels

In a metric setting, geodesics and autoparallels coincide, but in a metric-free framework with torsion, they are distinct. We therefore adopt autoparallels–curves whose tangent u is parallel transported by the full intrinsic connection (6b), $\Gamma^a{}_b$–as the natural trajectories of spinless test bodies:

$$\iota_u\,(\mathrm{D}u^a) = 0\,. \tag{149}$$

This condition is equivalent in Eulerian, Lagrangian, and intrinsic coframes, since the three connections are related by (6a)–(6c).

11.1. Eulerian description

Parametrizing worldlines by Eulerian time t, with velocity $v^i = \mathrm{d}x^i/\mathrm{d}t$, the autoparallel condition yields

$$D_t v^i = -c^2\,\Gamma^i{}_{00} - 2c\,v^j\,\Gamma^i{}_{(0j)} + v^i\left[c\,\Gamma^0{}_{00} + 2\,\Gamma^0{}_{(0j)}\,v^j\right] + \cdots, \tag{150}$$

where $D_t \equiv \partial_t + v^j\,\nabla_j$ denotes the material time derivative.

In the Newtonian limit we impose $D_t v^i = -g^i$, making the identification $g^i = c^2\,\Gamma^i{}_{00}$. Thus, gravitational acceleration is carried directly by the Eulerian connection components $\Gamma^i{}_{00}$ without the need for a gravitational potential. This description of gravitational acceleration complements the identification $g_i = c^2\,\iota_u\kappa^0{}_i$ introduced in section 8 in connection with Newton's law of gravitation. The subleading terms in (150) reproduce the Lense–Thirring contributions (Lense and Thirring 1918).

11.1.1. Metric comparison

If one introduces a reconstructed metric (16), then its temporal component satisfies $g_{00} \simeq -(1 + 2\Phi/c^2)$ in the weak-field limit, with Φ the Newtonian potential. Hence $\Gamma^i{}_{00} = \frac{1}{2}\,g^{ij}\,\partial_j g_{00}$ reproduces the same gravitational acceleration $g^i = c^2\,\Gamma^i{}_{00}$, confirming that the potential description of Newtonian gravity arises only when a metric is reconstructed *a posteriori* from the coframe.

11.2. Lagrangian and intrinsic descriptions

In Lagrangian coordinates, the autoparallel condition simplifies to $\iota_u(\mathrm{D}u^{\mu'}) = \Gamma^{\mu'}{}_{00} = 0$. In the intrinsic coframe, the Newtonian contributions from the Eulerian connection and the spin-bend-twist connection cancel, leaving

$$\Gamma^i{}_{00}\big|_{\text{intrinsic}} = 0\,. \tag{151}$$

Thus, in the Newtonian limit, the intrinsic autoparallel condition reduces to

$$\iota_u\left(\mathrm{d}u^i\right) = 0\,, \tag{152}$$

consistent with classical free fall.

Hence, the autoparallel construction reproduces Newton's law at leading order and yields the correct post-Newtonian corrections, while showing that in an intrinsic u-adapted coframe, the Newtonian gravitational force is entirely encoded in the defect geometry.

12. Discussion

This discussion section serves two main purposes. First, it aims to clarify the dynamical aspects of the minimal sector examined here, specifically focusing on the degrees of freedom and nonlinear stability. Second, it summarizes how the intrinsic defect formulation relates to observational interfaces, either directly through holonomy and flux or via metric-comparison reconstruction.

12.1. Degrees of freedom and nonlinear stability

A natural question to consider is whether the metric-free defect formulation preserves the same physical degrees of freedom as GR and whether its resulting dynamics remain stable beyond the linearized regime. While a comprehensive nonlinear constraint and Hamiltonian analysis is beyond the scope of this paper, we can clearly outline a few points regarding the minimal sector we have analyzed here.

Gauge structure. The fundamental fields can be represented as either $(\varphi^\mu, \psi^a{}_\mu)$ or, equivalently, $(\beta^a, \kappa^a{}_b)$. These fields exhibit the standard redundancies associated with a connection-based formulation: (i) Spacetime diffeomorphisms, which involve reparameterizations of motion and coordinates. (ii) Local frame transformations, which refer to changes in the internal basis affecting the coframe and the connection. These gauge freedoms help to define equivalence classes of field configurations. Physical quantities are represented by gauge-invariant flux or holonomy quantities, and when a metric is reconstructed for comparison, these can also provide derived metric outputs.

Minimal vacuum sector and propagating modes. The main findings of this paper focus on the defect-free exterior sector, where the conditions $\Sigma^a = 0$ and $\Lambda^a{}_b = 0$ hold, along with a vanishing $\Pi^a{}_b$ in the highlighted solutions. Additionally, we impose the condition of torsionlessness, $T^a = 0$, on the full coframe connection.

Table 3. Possible phenomenological interfaces of the metric-free defect formulation. The right column lists derived comparison outputs.

Signature	Intrinsic (metric-free)	Metric-comparison output
Gravitational waves	Wave solutions in $(\beta^a, \kappa^a{}_b)$ (section 7)	c, two transverse polarizations; waveform templates
Newtonian limit	$\rho_{\text{geom}} = \iota_{e_i}\iota_u\Theta^i{}_0$ (section 8)	Poisson limit; M calibration
Black hole exteriors	Defect-strength normalization; horizon diagnostics (section 10.7)	Schwarzschild/Kottler; A, (and κ_{sg} if included)
Defect holonomy	Loop/surface integrals of $\kappa^a{}_b$, $\Lambda^a{}_b$ around cores	Derived lensing / time-delay / phase shifts (via metric comparison)
Extensions	Modified capacity $L = \epsilon f(\Lambda)$ (section 9.4)	Potential departures (not developed here)

In this sector, the vacuum exteriors–such as Schwarzschild and Kottler solutions–are determined by symmetry and the Bianchi identities. When expressed through the metric-comparison interface, the radiative sector effectively reproduces the well-known two transverse gravitational-wave polarizations characteristic of GR.

Where additional modes could enter. Additional propagating degrees of freedom can only arise if one enlarges the dynamical sector beyond what is treated in the present paper, for example, by: (i) allowing independent propagating torsion/nonmetricity sectors (or a more general invariant constitutive choice), or (ii) introducing generalized capacities such as $f(\Lambda)$-type extensions. Such extensions are well-motivated directions for future work, but require a dedicated constraint analysis to determine whether extra modes are physical or gauge, and whether any additional modes are stable.

Nonlinear stability: scope of the present results. In the minimal sector studied here, the metric reconstruction provides a direct interface to the standard GR characterization of perturbations and stability for the corresponding vacuum solutions. Accordingly, the present paper should be read as establishing a controlled, metric-free formulation whose minimal vacuum and radiative sectors reproduce the familiar GR behavior at the level of comparison outputs, while leaving a full nonlinear constraint analysis of enlarged defect sectors and their cosmological applications to future work.

12.2. Possible phenomenology

This section summarizes potential observational interfaces of the metric-free defect formulation. Table 3 is organized in terms of *comparison outputs* that can be expressed in conventional metric language when desired ('Metric Comparison'), and as *intrinsic observables* naturally associated with defects (holonomy/flux-type measurements). The purpose is not to claim established deviations from GR in the minimal model developed here, but to delineate falsifiable targets for future analysis and for controlled extensions (e.g. generalized $f(\Lambda)$ sectors).

Several concrete directions follow from table 3:

1. *Wave-sector consistency tests.* The linearized sector predicts propagation at speed c with two transverse polarizations; deviations (if any) would arise only in controlled extensions or in defect-core scattering problems.
2. *Holonomy-based defect detection.* Because defects are characterized by incompatibility and distributional curvature/torsion, natural observables are loop/surface integrals that detect nontrivial holonomy/flux around defect cores. This provides a direct operational meaning to defect strength, analogous to defect measurement in continua.
3. *Strong-field comparisons via black-hole diagnostics.* The exterior solutions provide a benchmark set of observables (e.g. horizon area and, once included, surface gravity) that can be compared to standard GR templates, while remaining derived rather than assumed.
4. *Controlled departures beyond the minimal sector.* If one seeks phenomenology beyond GR in the Newtonian or cosmological regimes, it must arise from explicit extensions of the intrinsic Lagrangian capacity (e.g. $f(\Lambda)$), accompanied by stability and degree-of-freedom analyses.

13. Conclusion

We have formulated a theory of gravitation without a metric tensor. The fundamental gauge variables are the motion field φ^μ and the intrinsic deformation field $\psi^a{}_\mu$, which induce the velocity-distortion coframe $\beta^a = \psi^a{}_\mu \, \mathrm{d}\varphi^\mu$ and the spin-bend-twist connection $\kappa^a{}_b = \psi^a{}_\mu \, \mathrm{d}(\psi^{-1})^\mu{}_b$. Their intrinsic field strengths are $\Sigma^a = \mathrm{d}\beta^a + \kappa^a{}_b \wedge \beta^b$ and $\Lambda^a{}_b = \mathrm{d}\kappa^a{}_b + \kappa^a{}_c \wedge \kappa^c{}_b$. Gravitational phenomena emerge from the intrinsic field equations $\Sigma^a = \alpha^a$ and $\Lambda^a{}_b = \Theta^a{}_b$, which balance geometry against geometric incompatibilities: dislocations α^a and disclinations $\Theta^a{}_b$. The Newtonian limit of the time-space field equations yields mass density as the scalar contraction of time-space disclinations, showing that mass-energy arises directly from geometry within the defect-gravity sector developed here.

This geometric identification of mass as disclination density shifts the framework from postulated *stress-energy sources* to emergent defect-supported dynamics. Gravitational sources appear as manifestations of incompatibility within spacetime's intrinsic structure, and distributional sources are interpreted as idealized geometric defects, representing the singular limit of regularized defect cores. In this metric-free formulation, no scalar gravitational potential exists; gravitational accelerations are carried instead by the time-space components of the connection.

The framework reproduces key vacuum predictions of GR within the scope analyzed here. In the linearized regime considered here, gravitational waves propagate at the characteristic speed c with two transverse polarizations, and the Schwarzschild exterior emerges from spherically symmetric, torsion-free compatibility conditions. The Newtonian limit yields Poisson's equation for the gravitational field. Natural generalizations of the intrinsic Lagrangian, $L = \epsilon f(\Lambda)$, parallel $f(R)$ models; such extensions provide a controlled avenue for exploring departures from the minimal sector $L = \epsilon\Lambda$, but their phenomenology is not developed in the present paper.

Most significantly, this formulation reveals gravitation as a manifestation of *geometric incompatibility*. In the minimal gravity (defect) sector treated here, sources are not introduced as external stress-energy, but arise as regions where the spacetime structure fails to fit together smoothly–a time-space disclination in the fabric of spacetime itself. Einstein's postulate that matter *equals* geometry is replaced with the idea that matter *is* geometry in this geometric-incompatibility sense.

This geometric identification of matter as disclination density provides a natural bridge between macroscopic gravitation and microscopic structure, suggesting that spacetime's geometrical defects may underlie phenomena conventionally attributed to matter.

Limitations and outlook

Matter couplings. As mentioned in the Introduction, this paper develops the metric-free gravitational defect sector and its associated vacuum exteriors. The explicit coupling to standard matter fields—such as Maxwell fields, Dirac fields, and fluids—will be addressed in future work.

We envisage two consistent coupling routes: (A) an *interface* route in which standard matter fields couple to a reconstructed metric used only for comparison with conventional field theory, and (B) a *premetric/constitutive* route in which matter couples directly to $(\beta^a, \kappa^a{}_b)$ through constitutive tensors, postponing metric reconstruction. Route (A) would couple Maxwell, Dirac, or fluid stress tensors to $g_{\mu\nu}$, maintaining compatibility with standard field theory while treating the metric as a comparison device. Route (B) would express electromagnetic and matter constitutive relations directly in terms of the coframe basis, following premetric approaches (Hehl and Obukhov 2003). Developing either route in full generality is substantial and is deferred to follow-on work.

Cosmology and dark sector. While dark matter and dark energy inspire the exploration of alternative gravitational theories, the minimal model presented here does not claim to resolve these cosmological issues on its own. Instead, it offers a coherent metric-free foundation from which controlled extensions—such as generalized $f(\Lambda)$ sectors—can be explored. Notably, since the recovered Newtonian limit resembles GR, we do not claim that this paper provides a solution for galaxy rotation curves or MOND-like phenomenology (e.g. Famaey and McGaugh 2012) without the incorporation of additional model components. A logical next step is to examine controlled extensions, such as generalized $f(\Lambda)$ sectors, along with their homogeneous and isotropic reductions and stability properties.

Defect cores and singular idealizations. The description of the distributional defect should be regarded as an idealization of a regularized core: in a smooth core model, invariants remain finite; however, in the singular limit, local blow-up can occur even when integrated observables (such as holonomy or flux) remain well-defined.

The metric-free framework thus reframes gravitation as an intrinsic property of spacetime geometry. Where GR requires both geometry and external stress-energy, here all dynamics arise from the incompatibility conditions encoded by the induced fields $(\beta^a, \kappa^a{}_b)$ (equivalently, by singularities in the gauge potentials $(\varphi^\mu, \psi^a{}_\mu)$). Within its present scope, this approach may remain valid beyond the metric domain, offering new insights into defect-based gravitational sources and their metric comparison limits, and providing a platform for future work on matter couplings and cosmological extensions.

Data availability statement

No new data were created or analysed in this study.

Acknowledgments

The insightful comments and suggestions from two anonymous reviewers greatly enhanced the manuscript. I am grateful to my Princeton physics colleagues, Frans Pretorius and Paul Steinhardt, for their valuable comments and feedback on this theory. I also appreciate the conversations with David Al-Attar regarding de Rham currents.

Funding

This work was not supported by any funding agency.

Author contributions

This is the work of a single author.

Appendix A. 4D Spacetime defects and de Rham currents

In this appendix, we construct the hierarchy of Dirac-type distributions associated with submanifolds of spacetime–hypersurfaces (3D), surfaces (2D), lines (1D), and points (0D)—in the language of differential forms and de Rham currents (De Rham 1955), framed within the theory of generalized functions (Schwartz 1950, Gelfand and Shilov 1964). This generalizes the treatment of delta functions on lower-dimensional subsets from deWit's treatment of material defects in 3D (deWit 1973, appendix B) to four-dimensional spacetime. This construction forms the foundation for describing localized sources in gauge and gravity theories as idealized submanifold defects.

Let M be a smooth oriented 4D manifold (spacetime), and let $\Sigma \subset M$ be a smooth oriented submanifold of codimension k (not to be confused with the torsion 2-forms Σ^a). The Dirac current δ_Σ is defined via the pairing

$$\delta_\Sigma[\omega] = \int_\Sigma \omega\,, \qquad \omega \in \Omega_c^{4-k}(M)\,, \tag{153}$$

so δ_Σ is a degree-$(4-k)$ current (the integration current over Σ).

Equivalently, (we do not distinguish between the integration current and its Poincaré-dual delta form) we also write δ_Σ for the distributional k-form characterized by

$$\int_M \alpha \wedge \delta_\Sigma = \int_\Sigma \alpha\,, \qquad \alpha \in \Omega_c^{4-k}(M)\,. \tag{154}$$

With this convention,

$$\mathrm{d}\delta_\Sigma = \delta_{\partial\Sigma}\,. \tag{155}$$

Identifying δ_Σ with a distributional k-form uses only the orientation and wedge pairing; no metric or Hodge dual enters. This matches the 'capacity' viewpoint used in the main text.

A.1. Hierarchy of currents and boundary operators

Starting with a compact 4D region Ω, this establishes a complete differential cascade:

$$\mathrm{d}\delta_\Omega = \delta_V\,, \quad \text{where } \partial\Omega = V \quad (\text{3D hypersurface})\,, \tag{156a}$$

$$\mathrm{d}\delta_V = \delta_S\,, \quad \text{where } \partial V = S \quad (\text{2D surface})\,, \tag{156b}$$

$$\mathrm{d}\delta_S = \delta_L\,, \quad \text{where } \partial S = L \quad (\text{1D curve})\,, \tag{156c}$$

$$\mathrm{d}\delta_L = \sum_{P\in\partial L} \sigma(P)\,\delta_P\,, \quad \text{where } \partial L \text{is a finite set of endpoints } P \quad (\text{0D points})\,, \tag{156d}$$

with $\sum_P \sigma(P) = 0$ on a closed, boundaryless M.

On a closed (compact, boundaryless) manifold M, the endpoint 'charge neutrality' follows directly from the current boundary operator: testing (156*d*) against the constant 0-form 1 gives

$$0 = (\mathrm{d}\delta_L)[1] = \delta_L[\mathrm{d}1] = \sum_{P\in\partial L} \sigma(P)\,\delta_P[1] = \sum_{P\in\partial L} \sigma(P)\,, \tag{157}$$

since $\mathrm{d}1 = 0$. Equivalently, this is the statement that the total boundary of a boundary vanishes in the de Rham current complex.

Thus, a 4D region Ω induces a hierarchy: a 3D hypersurface current δ_V, which may have a 2D surface boundary S, which may have a 1D curve boundary L, terminating at 0D endpoints P.

A.2. Closed versus open submanifolds

For any closed submanifold Σ (i.e. $\partial\Sigma = \emptyset$), equation (155) yields:

$$\mathrm{d}\delta_\Sigma = 0\,. \tag{158}$$

This means the delta current δ_Σ is closed. In particular:

- If V is a closed hypersurface ($\partial V = \emptyset$), then $\mathrm{d}\delta_V = 0$,
- If S is a closed surface ($\partial S = \emptyset$), then $\mathrm{d}\delta_S = 0$,
- If L is a closed curve ($\partial L = \emptyset$), then $\mathrm{d}\delta_L = 0$.

A.3. Controlled regularization and current limits

The de Rham currents used in this appendix represent an idealized (singular) description of defect cores. To connect this idealization to smooth core models, we use a controlled *regularize-limit* procedure, consistent with section 4.4: all fields are smooth for each $\varepsilon > 0$, so all wedge products are classical, and only after computations at fixed ε do we take the defect limit in the sense of currents.

Controlled regularization of a defect core. Let $C \subset M$ be the defect support (e.g. a timelike worldsheet). A regularized core is a one-parameter family of smooth fields $(\varphi_\varepsilon, \psi_\varepsilon)$–hence $(\beta^a_\varepsilon, \kappa^a{}_{b,\varepsilon})$–such that: (i) on $M \setminus C$ the fields converge smoothly as $\varepsilon \to 0$ (uniformly with all derivatives on compact sets), and (ii) the field strengths $(\Sigma^a_\varepsilon, \Lambda^a{}_{b,\varepsilon})$ concentrate onto C with finite total strength. The limiting defect sources are then defined by testing against smooth compactly supported forms. For example, we write $\Lambda^a{}_{b,\varepsilon} \rightharpoonup \Theta^a{}_b$ as $\varepsilon \to 0$ if for every test 2-form $\omega \in \Omega^2_c(M)$ one has

$$\int_M \omega \wedge \Lambda^a{}_{b,\varepsilon} \;\longrightarrow\; \Theta^a{}_b[\omega]\,, \tag{159}$$

and similarly $\Sigma^a_\varepsilon \rightharpoonup \alpha^a$. In this way, defect-supported curvature and torsion arise as the singular limits of smooth cores, without undefined products of distributions.

Spherical mass calibration (outline). On a spatial slice Σ_T, let P be the intersection point of the timelike defect worldsheet with the slice. Choose a smooth, compactly supported family $\rho_{\mathrm{geom},\varepsilon}$ in a shrinking neighborhood of P, normalized so that for any domain V containing P the total geometric mass is fixed:

$$\int_V \rho_{\mathrm{geom},\varepsilon}\,\hat{\epsilon} = -\frac{4\pi G}{c^2} M \qquad \text{for all sufficiently small } \varepsilon\,. \tag{160}$$

Solving the metric-free Gauss law (79) then yields an exterior acceleration flux $\hat{g}_\varepsilon$ such that, for any fixed domain V with $P \in V$ and $\mathrm{supp}(\rho_{\mathrm{geom},\varepsilon}) \subset V$ (i.e. for all sufficiently small ε), Stokes' theorem implies

$$\int_{\partial V} \hat{g}_\varepsilon = -c^2 \int_V \rho_{\mathrm{geom},\varepsilon}\,\hat{\epsilon}\,, \tag{161}$$

and therefore the boundary flux $\int_{\partial V} \hat{g}_\varepsilon$ is independent of ε.

A.4. Spacetime defect theory and distributional geometry

The theory of material defects has a long history, dating back to the work of Weingarten (1901) and Volterra (1907), and was formalized by deWit and others (e.g. Mura 1963, 1982, deWit 1973, Kossecka and deWit 1977, Edelen and Lagoudas 1988, Kleman and Friedel 2008). It provides a robust geometric framework for describing dislocations and disclinations as manifestations of incompatibility in elastic media. Weingarten's theorem relates closure failures around irreducible cycles to jumps in displacement and rotation fields, whereas deWit's canonical defect densities generalize these ideas to continuum theories.

Our goal is to expand this framework into four-dimensional spacetime by substituting classical displacement and rotation with the motion field $\varphi^\mu(X^{\mu'})$ and the intrinsic deformation field $\psi^a{}_\mu(X^{\mu'})$. This formulation is geometrically natural, does not necessitate the introduction of a metric, and allows for the accommodation of gravitational sources as topological and geometric defects within spacetime itself.

A.4.1. Weingarten's theorem

Let $\Sigma \subset M$ be a smooth, oriented 3D hypersurface in spacetime. If a field $f \in C^1(M \setminus \Sigma)$ has a jump discontinuity $[\![f]\!]$ across Σ, then its distributional derivatives satisfy:

$$\mathrm{d}f = \widetilde{\mathrm{d}f} + [\![f]\!]\,\delta_\Sigma\,, \tag{162a}$$

$$\mathrm{d}^2 f = \mathrm{d}\left([\![f]\!]\,\delta_\Sigma\right) = \left(\mathrm{d}_{||}\,[\![f]\!]\right)\wedge\delta_\Sigma + [\![f]\!]\,\delta_{\partial\Sigma}\,, \tag{162b}$$

where $\widetilde{\mathrm{d}f}$ denotes the smooth part, and $\mathrm{d}_{||}$ denotes the tangential exterior derivative along Σ, acting on the one-sided (or averaged) trace of the jump function; this avoids ill-defined products and keeps covariance manifest[9]. Here δ_Σ is the Dirac current associated with Σ, and $\delta_{\partial\Sigma}$ is its exterior derivative supported on the boundary $\partial\Sigma$.

If $[\![f]\!]$ is constant along Σ, as in Weingarten's theorem, then the term $(\mathrm{d}_{||}\,[\![f]\!])\wedge\delta_\Sigma$ vanishes, and the second derivative reduces to a pure line source:

$$\mathrm{d}^2 f = [\![f]\!]\,\delta_{\partial\Sigma}\,, \tag{163}$$

which matches the expressions for line dislocations and disclinations in deWit (1973), equations 5.19 and 5.20. However, in the general case $[\![f]\!]$ may vary along Σ, and the surface defect density current $(\mathrm{d}_{||}\,[\![f]\!])\wedge\delta_\Sigma$ is a 2-current supported on the 3D hypersurface Σ that measures the non-uniformity of the jump discontinuity.

A.4.2. Distributional sources

Let φ^μ and $\psi^a{}_\mu$ be motion and intrinsic deformation fields with jump discontinuities across one or more hypersurfaces $\Sigma \subset M$. For an ordinary 0-form f with a jump $[\![f]\!]$ across Σ, the generalized Weingarten formulas give (162a) and (162b). Applying this to the motion field φ^μ yields

$$\mathrm{d}^2\varphi^\mu = \left(\mathrm{d}_{||}\,[\![\varphi^\mu]\!]\right)\wedge\delta_\Sigma + [\![\varphi^\mu]\!]\,\delta_{\partial\Sigma}\,. \tag{164}$$

The corresponding dislocation 2-forms (12) are

$$\alpha^a = \psi^a{}_\mu\,\mathrm{d}^2\varphi^\mu = \left(\mathscr{D}_{||}\,[\![\varphi^a]\!]\right)\wedge\delta_\Sigma + [\![\varphi^a]\!]\,\delta_{\partial\Sigma}\,, \tag{165}$$

where $[\![\varphi^a]\!] = \psi^a{}_\mu\,[\![\varphi^\mu]\!]$ and the identity

$$\psi^a{}_\mu\,\mathrm{d}_{||}\,[\![\varphi^\mu]\!] = \mathscr{D}_{||}\,[\![\varphi^a]\!] \tag{166}$$

holds along Σ, where $\mathscr{D}_{||}$ denotes the exterior covariant derivative *tangential to* Σ, obtained from $\mathscr{D}$ by pulling back the regular (one-sided or averaged) trace of the connection $\kappa^a{}_b$ to Σ. This ensures that the derivative of $[\![\varphi^a]\!]$ is taken in a frame-covariant manner without introducing ill-defined products of distributions.

For disclinations, we consider the geometric combination $(\psi^{-1})^\mu{}_b\,\mathrm{d}^2\psi^a{}_\mu$ of (13), which involves incompatibilities in $\mathrm{d}^2\psi^a{}_\mu$ and $(\psi^{-1})^\mu{}_a$. Using the Weingarten formulas for $\psi^a{}_\mu$ gives the distributional structure

$$\left(\psi^{-1}\right)^\mu{}_b\,\mathrm{d}^2\psi^a{}_\mu \;=\; \left(\psi^{-1}\right)^\mu{}_b\left[\mathscr{D}_{||}\,[\![\psi^a{}_\mu]\!]\wedge\delta_\Sigma + [\![\psi^a{}_\mu]\!]\,\delta_{\partial\Sigma}\right]\,, \tag{167}$$

[9] One-sided traces are the limits $\lim_{\epsilon\to 0^+} f(x\pm\epsilon)$ approaching Σ from either side, while averaged traces are $\frac{1}{2}(f^+ + f^-)$. Both definitions avoid ill-defined products of distributions and preserve the covariant structure of differential forms.

Table 4. Classification of 4D defects based on the index structure of dislocations $\alpha^a = \frac{1}{2}\,\alpha^a{}_{bc}\,\beta^b \wedge \beta^c$ and disclinations $\Theta^a{}_b = \frac{1}{2}\,\Theta^a{}_{bcd}\,\beta^c \wedge \beta^d$. This classification extends the classical 3D material defect taxonomy (Volterra, deWit, Kröner) to four-dimensional spacetime.

Type	Components	Index condition	Interpretation
Edge	$\alpha^a{}_{bc}$	$a \neq b,\, a \neq c$	Slip $\perp$ defect plane
Screw	$\alpha^a{}_{bc}$	$a = b$ or $a = c$	Slip $\parallel$ defect plane
Wedge	$\Theta^a{}_{bcd}$	$a = c,\, a = d,\, b = c,$ or $b = d$	Rotation axis in slip plane
Twist	$\Theta^a{}_{bcd}$	$a \neq c,\, a \neq d, b \neq c,\, b \neq d$	Rotation axis orthogonal to plane

where the derivative $\mathscr{D}_{\|}\,[\![\psi^a{}_\mu]\!]$ insures proper invariance of the derivative along Σ. Since $\psi^a{}_\mu$ is piecewise C^1 with bounded jump and $(\psi^{-1})^\mu{}_b$ is the piecewise smooth inverse, the term $(\psi^{-1})^\mu{}_b\,\mathrm{d}^2\psi^a{}_\mu$ is well-defined as a current via one-sided traces along Σ. Thus, the disclination 2-forms (13) are

$$\Theta^a{}_b = -\left(\mathscr{D}_{\|}\,[\![\psi^a{}_b]\!]\right) \wedge \delta_\Sigma - [\![\psi^a{}_b]\!]\,\delta_{\partial\Sigma}\,, \tag{168}$$

where

$$[\![\psi^a{}_b]\!] \equiv \left(\psi^{-1}\right)^\mu{}_b\,[\![\psi^a{}_\mu]\!]\,. \tag{169}$$

This ensures the jump is expressed in a frame-covariant manner.

If the jumps $[\![\varphi^a]\!]$ and $[\![\psi^a{}_b]\!]$ are constant along Σ, the surface terms vanish and the defect densities reduce to line sources supported on $\Gamma = \partial\Sigma$:

$$\alpha^a = [\![\varphi^a]\!]\,\delta_\Gamma\,, \tag{170a}$$

$$\Theta^a{}_b = -\,[\![\psi^a{}_b]\!]\,\delta_\Gamma\,. \tag{170b}$$

In 3D, these match the canonical line defect sources derived by deWit (1973).

Coarse-graining to volumetric sources. Beyond idealized sharp cuts, we allow $\Theta^a{}_b$ to carry both a smooth (volumetric) part in the bulk and singular parts supported on lower-dimensional submanifolds (surfaces or lines) (e.g. Evans and Gariepy 1992, Federer 1996, Ambrosio *et al* 2000). The smooth contribution is a genuine 2-form on M, and its time-space contraction $\iota_{e_i}\iota_u\Theta^i{}_0$ is precisely the density field that appears in (71), thereby defining mass as a distributed incompatibility of the intrinsic deformation. The singular parts coexist with this volumetric component and represent embedded line or surface defects within matter, in direct analogy with classical dislocation/disclination theory.

A.4.3. Classification

Using the decompositions

$$\alpha^a = \tfrac{1}{2}\,\alpha^a{}_{bc}\,\beta^b \wedge \beta^c\,, \tag{171a}$$

$$\Theta^a{}_b = \tfrac{1}{2}\,\Theta^a{}_{bcd}\,\beta^c \wedge \beta^d\,, \tag{171b}$$

we classify spacetime dislocations and disclinations in direct analogy with their classical three-dimensional counterparts, now extended to 4D.

Dislocations. These represent translational incompatibilities sourced by discontinuities in the motion field φ^μ. The classification depends on the index structure of $\alpha^a = \frac{1}{2}\,\alpha^a{}_{bc}\beta^b \wedge \beta^c$:

- *Edge dislocation:* $a \neq b$ and $a \neq c$
  The Burgers vector is transverse to the defect plane spanned by b and c.
- *Screw dislocation:* $a = b$ or $a = c$
  The Burgers vector lies in the defect plane; that is, the dislocation line is helical.

Disclinations. These arise from rotational discontinuities in the frame field $\psi^a{}_\mu$, and the classification is similarly governed by the relationship between the rotation indices a, b and the cut plane c, d in $\Theta^a{}_b = \frac{1}{2}\,\Theta^a{}_{bcd}\,\beta^c \wedge \beta^d$:

- *Wedge disclination:* $a = c,\ a = d,\ b = c,$ or $b = d$
  The Frank vector is tangential to the slip plane–rotation occurs about an axis lying in the plane.
- *Twist disclination:* $a \neq c, a \neq d, b \neq c$ and $b \neq d$
  The Frank vector is normal to the slip plane–rotation axis is orthogonal to the cut.

Table 4 classifies 4D dislocations and disclinations based on their index structure.

Appendix B. Black hole extensions

This section establishes a clear correspondence between a smooth, regularized defect core and the torsionless Schwarzschild/Kottler exterior discussed in section 10. In the context of GR, the careful application of singular limits of smooth families is a common practice, particularly in the setting of distributional curvature (e.g. Geroch and Traschen 1987). We will begin our analysis in the areal gauge defined by $C(R) = R$ to ensure the construction remains straightforward.

Exterior region. The matching construction uses the exterior mass parameter M, whose value is fixed by the Gauss-law flux relation between the integrated time-space disclination strength and the physical mass, as discussed in section 8, culminating in equation (130). This appendix focuses only on the smooth interior/exterior interface. Given M, define the Schwarzschild exterior coframe on the static domain $R > R_{\mathrm{H}} = 2GM/c^2$ by (132):

$$\beta^0_{\mathrm{ext}} = A_{\mathrm{ext}}(R)\,\mathrm{d}T, \qquad \beta^1_{\mathrm{ext}} = \frac{1}{A_{\mathrm{ext}}(R)}\,\mathrm{d}R, \qquad \beta^2_{\mathrm{ext}} = R\,\vartheta^2, \qquad \beta^3_{\mathrm{ext}} = R\,\vartheta^3, \tag{172}$$

with $A^2_{\mathrm{ext}}(R) = 1 - \frac{2GM}{c^2 R}$ (and similarly for Kottler, if desired). On this domain, the torsionless connection coefficients are those of section 10, in particular $\Gamma^0{}_1 = D\beta^0$ with $D = A'/(AB)$, which reduces to $D = A'$ for the Schwarzschild/Kottler exterior where $B = 1/A$.

Choice of matching radius. Choose any matching radius $R_m > R_{\mathrm{H}}$. On $R \geqslant R_m$ we work in the same GR-compatible exterior sector as in section 10: $\Sigma^a = \Lambda^a{}_b = \Pi^a{}_b = 0$, $T^a = 0$, and $q_{ab} = 0$.
Interior (regularized) defect model specified by disclination strength. To exhibit an explicit interior/exterior matching for a given time-space wedge disclination strength, we prescribe a smooth, spherically symmetric regularization of the scalar disclination density on a spatial slice,

$$\rho_{\mathrm{geom},\varepsilon}(R) \;\equiv\; \iota_{e_i}\iota_u \Theta^i{}_{0,\varepsilon}\,, \tag{173}$$

supported in $0 \leqslant R < R_m$. Let $V = B_{R_m}(P) \subset \Sigma_T$ denote the areal-radius ball about P. Then the normalization (160) reads

$$\int_V \rho_{\mathrm{geom},\varepsilon}\,\hat{\epsilon} = \int_0^{R_m} \rho_{\mathrm{geom},\varepsilon}(R)\,4\pi R^2\,\mathrm{d}R = -\frac{4\pi G}{c^2}M, \tag{174}$$

for any domain V containing the core[10]. (For a smooth core, it is sufficient that $\rho_{\mathrm{geom},\varepsilon}$ remain bounded as $R \to 0$, so that $m_\varepsilon(R) = O(R^3)$ and hence $A^2_{\mathrm{int}}(R) \to 1$ as $R \to 0$.) In the GR-compatible torsionless branch used here, with $u = \partial_T$ and $B = 1/A$, one has $\hat{\epsilon} = \iota_u \epsilon = (AB)R^2\,\mathrm{d}R \wedge \mathrm{d}\gamma = R^2\,\mathrm{d}R \wedge \mathrm{d}\gamma$, so the radial reduction in (174) indeed yields $4\pi R^2\,\mathrm{d}R$.

Equivalently, introduce the enclosed mass function

$$m_\varepsilon(R) \;\equiv\; -\frac{c^2}{4\pi G}\int_0^R \rho_{\mathrm{geom},\varepsilon}(r)\,4\pi r^2\,\mathrm{d}r, \tag{175}$$

so that $m_\varepsilon(0) = 0$ and $m_\varepsilon(R) = M$ for $R \geqslant R_m$.

Explicit matching calculation. In the areal gauge $C(R) = R$ and in the torsionless, Lorentz-reduced sector ($T^a = 0$, $q_{ab} = 0$), define the interior comparison profile by

$$A^2_{\mathrm{int}}(R) \;\equiv\; 1 - \frac{2G\,m_\varepsilon(R)}{c^2 R}, \tag{176}$$

and set $B_{\mathrm{int}} = 1/A_{\mathrm{int}}$; for Kottler subtract $\frac{\Lambda}{3}R^2$. By construction $A^2_{\mathrm{int}}(R_m) = A^2_{\mathrm{ext}}(R_m)$ since $m_\varepsilon(R_m) = M$. Moreover, if $\rho_{\mathrm{geom},\varepsilon}$ is chosen to vanish at R_m (e.g. by support strictly inside R_m), then $m'_\varepsilon(R_m) = 0$ and hence $A'_{\mathrm{int}}(R_m) = A'_{\mathrm{ext}}(R_m)$, so the coframe and the tangential pullback of the torsionless spin connection match continuously across $S^2(R_m)$ and no spurious δ-supported shell is introduced at the matching sphere.

If one prefers an explicit C^1 interface independent of such endpoint conditions, one may alternatively impose $A_{\mathrm{int}}(R_m) = A_{\mathrm{ext}}(R_m)$ and $A'_{\mathrm{int}}(R_m) = A'_{\mathrm{ext}}(R_m)$ using a short matching layer (e.g. a cubic Hermite interpolation for A or A^2) without altering the integrated defect strength (174).

[10] Many distinct smooth profiles satisfy this normalization; the exterior depends only on the integrated strength.

Existence and (non-)uniqueness for fixed disclination strength. For any prescribed strength M and any smooth regularization $\rho_{\mathrm{geom},\varepsilon}$ satisfying (174), the construction above yields a smooth interior profile and a C^1 match to the Schwarzschild/Kottler exterior at R_m, hence an explicit existence result. The matching is unique at the level of exterior observables: the exterior mass parameter is fixed solely by the integrated defect strength (or equivalently by the Gauss-law flux/holonomy). The interior is not unique: many distinct smooth core regularizations share the same total disclination strength and therefore generate the same exterior geometry.

ORCID iD

Jeroen Tromp 0000-0002-2742-8299

References

Abbott B P *et al* 2016 Observation of gravitational waves from a binary black hole merger *Phys. Rev. Lett.* **116** 061102

Abbott B P *et al* 2017 GW170817: observation of gravitational waves from a binary neutron star inspiral *Phys. Rev. Lett.* **119** 161101

Abbott B P *et al* 2021 Tests of general relativity with binary black holes from the second LIGO-Virgo gravitational-wave transient catalog *Phys. Rev. D* **103** 122002

Abbott B P *et al* 2023 GWTC-3: compact binary coalescences observed by LIGO and Virgo during the second part of the third observing run *Phys. Rev. X* **13** 041039

Adak M, Dereli T, Kok E and Sert O 2025 Reformulation of continuum defects in terms of the general teleparallel geometry in the language of exterior algebra *Int. J. Theor. Phys.* **64** 99

Addazi A, Capozziello S, Marciano A and Meluccio G 2025 Gravity from pre-geometry *Class. Quantum Grav.* **42** 045012

Aldrovandi R and Pereira J G 2013 *Teleparallel Gravity: An Introduction* (Springer)

Ambrosio L, Fusco N and Pallara D 2000 *Functions of Bounded Variation and Free Discontinuity Problems (Oxford Mathematical Monographs)* (Oxford University Press)

Bahamonde S, Dialektopoulos K F, Escamilla-Rivera C, Farrugia G, Gakis V, Hendry M, Hohmann M, Said J L, Mifsud J and Valentino E D 2023 Teleparallel gravity: from theory to cosmology *Rep. Prog. Phys.* **86** 026901

Baldazzi A, Melichev O and Percacci R 2022 Metric-affine gravity as an effective field theory *Ann. Phys., NY* **438** 168757

Barceló C, Liberati S and Visser M 2011 Analogue gravity *Living Rev. Relativ.* **14** 3

Bertone G and Hooper D 2018 History of dark matter *Rev. Mod. Phys.* **90** 045002

Bilby B A and Smith E 1956 Continuous distributions of dislocations: III *Proc. R. Soc. A* **236** 481–505

Blagojević M and Hehl F W (ed) 2013 *Gauge Theories of Gravitation: A Reader With Commentaries* (Imperial College Press)

Capozziello S, Cianci R, Stornaiolo C and Vignolo S 2008 $f(R)$ cosmology with torsion *Phys. Scr.* **78** 065010

Capozziello S and Laurentis M D 2011 Extended theories of gravity *Phys. Rep.* **509** 167–321

Carneiro F, Ulhoa S, Maluf J and da Rocha-Neto J 2021 Non-linear plane gravitational waves as space-time defects *Eur. Phys. J. C* **81** 67

Cartan E 1922 Sur une généralisation de la notion de courbure de Riemann et les espaces à torsion *C. Rend. de l'Acad. des Sci.* **174** 593–5

Cartan E 1923 Sur les variétés à connexion affine et la théorie de la relativité généralisée *Ann. Sci. Éc. Norm. Supér.* **40** 325–412

Castillo-Felisola O, Grez B, Morocho-Lopez M, Perdiguero J, Skirzewski A, Vaca-Santana J and Zambra-Gomez N 2025 Polynomial affine model of gravity: after 10 years *Universe* **11** 102

Cattaneo A S and Schiavina M 2019 The reduced phase space of Palatini-Cartan-Holst theory *Ann. Henri Poincaré* **20** 445–80

Choquet-Bruhat Y, DeWitt-Morette C and Dillard-Bleick M 1982 *Analysis, Manifolds and Physics* Revised edn (North-Holland)

Collaboration P 2020 Planck 2018 results –VI. Cosmological parameters *Astron. Astrophys.* **641** A6

Cosserat E and Cosserat F 1907 Sur la mécanique générale *C. Rend. hebd. des Séances de l'Acad. des Sci.* **145** 1139

Cosserat E and Cosserat F 1909 *Théorie des Corps déformables* (A. Herman et Fils)

De Rham G 1955 *Variétés Différentiables* (Hermann) English version: Differentiable manifolds (Springer, 1984)

deWit R 1973 Theory of disclinations: II. Continuous and discrete disclinations in anisotropic elasticity *J. Res. Natl. Bur. Stand. (U.S.)* **77** 49–100

deWit R 1969 Linear theory of static disclinations *Fundamental Aspects of Dislocation Theory* vol 1, ed J A Simmons and R deWit pp 651–73

Di Valentino E, Mena O, Pan S, Visinelli L, Yang W, Melchiorri A, Mota D F, Riess A G and Silk J 2021 In the realm of the Hubble tension—a review of solutions *Class. Quantum Grav.* **38** 153001

Dudek M and Garecki J 2019 General relativity with a positive cosmological constant Λ as a gauge theory *Axioms* **8** 24

Edelen D G B and Lagoudas D C 1988 *Gauge Theory and Defects in Solids* (North-Holland)

Einstein A 1928 Riemann-Geometrie mit Aufrechterhaltung des Begriffes des Fernparallelismus *Sitzungsber. Preuss. Akad. Wiss. Phys. Math. Kl.* **17** 217

Eringen A 1999 *Microcontinuum Field Theories I: Foundations and Solids* (Springer)

Evans L C and Gariepy R F 1992 *Measure Theory and Fine Properties of Functions* (CRC Press)

Famaey B and McGaugh S S 2012 Modified newtonian dynamics (MOND): observational phenomenology and relativistic extensions *Living Rev. Relativ.* **15** 10

Federer H 1996 *Geometric Measure Theory* (Springer)

Frankel T 2011 *The Geometry of Physics: An Introduction* 3rd edn (Cambridge University Press)

Gelfand I M and Shilov G E 1964 *Generalized Functions, Volume I: Properties and Operations* (Academic)

Geroch R and Traschen J 1987 Strings and other distributional sources in general relativity *Phys. Rev. D* **36** 1017–31

Giaquinta M, Modica G and Souček J 1998 *Cartesian Currents in the Calculus of Variations* (Springer)

Hehl F W, McCrea J D, Mielke E W and Ne'eman Y 1995 Metric-affine gauge theory of gravity: field equations, Noether identities, world spinors and breaking of dilation invariance *Phys. Rep.* **258** 1–171

Hehl F W and Obukhov Y N 2003 *Foundations of Classical Electrodynamics: Charge, Flux and Metric* (Birkhäuser)

Hehl F W, von der Heyde P, Kerlick G D and Nester J M 1976 General relativity with spin and torsion: foundations and prospects *Rev. Mod. Phys.* **48** 393–416

Hohmann M, Krššák M, Pfeifer C and Ualikhanova U 2018 Propagation of gravitational waves in teleparallel gravity theories *Phys. Rev. D* **98** 124004

Holländer E F 1960 The basic equations of the dynamics of the continuous distribution of the dislocations III. Special problems *Czech. J. Phys. B* **10** 551–60

Holländer E. F. 1960 The basic equations of the dynamics of the continuous distribution of the dislocations I. General theory *Czech. J. Phys. B* **10** 409–418

Holländer E. F. 1960 The basic equations of the dynamics of the continuous distribution of the dislocations II. Interpretation of general theory *Czech. J. Phys. B* **10** 479–487

Hossenfelder S 2014 Theory and phenomenology of space-time defects *Adv. High Energy Phys.* **2014** 950672

Hossenfelder S and Gallego Torromé R 2018 General relativity with space-time defects *Class. Quantum Grav.* **35** 175014

Isi M, Giesler M, Farr W M, Scheel M A and Teukolsky S A 2019 Testing the no-hair theorem with GW150914 *Phys. Rev. Lett.* **123** 111102

Itin Y 2009 On light propagation in premetric electrodynamics: the covariant dispersion relation *J. Phys. A: Math. Theor.* **42** 475402

Jacobson T 1995 Thermodynamics of spacetime: the Einstein equation of state *Phys. Rev. Lett.* **75** 1260–3

Järv L, Rünkla M, Saal M and Vilson O 2018 Nonmetricity formulation of general relativity and its scalar-tensor extension *Phys. Rev. D* **97** 124025

Jiménez J B, Heisenberg L and Koivisto T S 2019 The geometrical trinity of gravity *Universe* **5** 173

Jiménez J B, Heisenberg L and Koivisto T 2018 Coincident general relativity *Phys. Rev. D* **98** 044048

Jiménez-Cano A, 2022, Metric-affine gauge theories of gravity: foundations and new insights.

Katanaev M O 2005 Geometric theory of defects *Phys. Usp.* **48** 675–701

Katanaev M and Volovich I 1992 Theory of defects in solids and three-dimensional gravity *Ann. Phys., NY* **216** 1–28

Kijowski J and Tulczyjew W M 1979 *A Symplectic Framework for Field Theories* vol 107 (Springer)

Kleinert H 1989 *Gauge Fields in Condensed Matter* (World Scientific)

Kleinert H 2008 *Multivalued Fields in Condensed Matter, Electromagnetism and Gravitation* (World Scientific)

Kleman M and Friedel J 2008 Disclinations, dislocations and continuous defects: a reappraisal *Rev. Mod. Phys.* **80** 61–115

Klinkhamer F R 2025 Big bang as spacetime defect *Mod. Phys. Lett. A* **40** 2530010

Kondo K 1952 On the geometrical and physical foundations of the theory of yielding *Proc. 2nd Japan Nat. Congr. App. Mech.* pp 41–47

Kondo K 1955 Non-Riemannian geometry of imperfect crystals from a macroscopic viewpoint *RAAG Memoirs 1 Div. D* **1** 458–69

Kondo K 1963 Non-Riemannian and Finslerian approaches to the theory of yielding *Int. J. Engng. Sci.* **1** 71–88

Kondo K 1964 On the analytical and physical foundations of the theory of dislocations and yielding by the differential geometry of continua *Int. J. Engng. Sci.* **2** 219–51

Kossecka E and deWit R 1977 Disclination kinematics *Arch. Mech.* **29** 633–51

Krantz S G and Parks H R 2008 *Geometric Integration Theory* (Birkhäuser)

Kröner E 1981 Continuum theory of defects *Phys. Defects (Les Houches, Session 35)* **35** 215–315

Krššák M, van den Hoogen R J, Pereira J G, Böhmer C G and Coley A A 2019 Teleparallel theories of gravity: illuminating a fully invariant approach *Class. Quantum Grav.* **36** 183001

Lazkoz R, Lobo F S N, Ortiz-Baños M and Salzano V 2019 Observational constraints of $f(Q)$ gravity *Phys. Rev. D* **100** 104027

Lense J and Thirring H 1918 Über den Einfluß der Eigenrotation der Zentralkörper auf die bewegung der planeten und monde nach der einsteinschen gravitationstheorie *Phys. Z.* **19** 156–63

Liberati S 2013 Tests of Lorentz invariance: a 2013 update *Class. Quantum Grav.* **30** 133001

Lieu R 2024 The binding of cosmological structures by massless topological defects *Mon. Not. R. Astron. Soc.* **531** 1630–6

MacDowell S W and Mansouri F 1977 Unified geometric theory of gravity *Phys. Rev. Lett.* **38** 739–42

Montesinos M, Romero R and Gonzalez D 2020 The gauge symmetries of $f(R)$ gravity with torsion in the Cartan formalism *Class. Quantum Grav.* **37** 045008

Mura T 1963 Continuous distribution of moving dislocation *Phil. Mag.* **8** 843–57

Mura T 1982 *Micromechanics of Defects in Solids* (Martinus Nijhoff Publishers, The Hague)

Noll W 1974 *The Foundations of Mechanics and Thermodynamics* (*Selected Papers*) (Springer)

Nye J F 1953 Some geometrical relations in dislocated crystals *Acta Metall.* **1** 153–62

Oriti D (ed) 2014 *Approaches to Quantum Gravity: Toward a New Understanding of Space, Time and Matter* (Cambridge University Press)

Padmanabhan T 2010 Thermodynamical aspects of gravity: new insights *Rep. Prog. Phys.* **73** 046901

Padmanabhan T 2012 Emergent perspective of gravity and dark energy *Res. Astron. Astrophys.* **12** 891

Peebles P J E and Ratra B 2003 The cosmological constant and dark energy *Rev. Mod. Phys.* **75** 559–606

Puntigam R A and Soleng H H 1997 Volterra distortions, spinning strings and cosmic defects *Class. Quantum Grav.* **14** 1129

Rigouzzo C and Zell S 2022 Coupling metric-affine gravity to a Higgs-like scalar field *Phys. Rev. D* **106** 024015

Schwartz L 1950 *Théorie des Distributions* (Hermann)

Sotiriou T P and Faraoni V 2010 $f(R)$ theories of gravity *Rev. Mod. Phys.* **82** 451–97

Trautman A 1973 On the structure of the Einstein-Cartan equations *Symp. Math.* **12** 139

Verlinde E P 2017 Emergent gravity and the dark Universe *SciPost Phys.* **2** 016

Volovik G E 2003 *The Universe in a Helium Droplet* (Oxford University Press)

Volterra V 1907 Sur l'équilibre des corps élastiques multiplement connexes *Ann. Sci. Ec. Norm. Super.* **24** 401–517

Weinberg S 1989 The cosmological constant problem *Rev. Mod. Phys.* **61** 1–23

Weingarten J 1901 Sulle superfici di discontinuita nella teoria dell'elasticita dei corpi solidi *Atti. Accad. Naz. Lincei, Cl. Sci. Fis. Mat. Natur. Rend.* **10** 57–60

Wise D K 2010 Macdowell-Mansouri gravity and Cartan geometry *Class. Quantum Grav.* **27** 155010